Decadal Variability in the Northeast Pacific in a Physical-Ecosystem Model: The Role of Mixed Layer Depth and Trophic Interactions

Michael Alexander[a], Antonietta Capotondi[a], Arthur Miller[b], Fei Chai[c], Richard Brodeur[d], Clara Deser[e], Doug Neilson[b], and Jon Eischeid[a]

a NOAA, Earth System Research Laboratory, Boulder, CO 80305, USA

b Scripps Institution of Oceanography, University of California, San Diego, La Jolla, CA 92093, USA

c School of Marine Sciences, University of Maine, Orono, ME 04469, USA

d NOAA, Northwest Fisheries Science Center, Hatfield Marine Science Center Newport, OR 97365 USA

e NCAR/Climate and Global Dynamics Division, Boulder, CO 80307, USA

Submitted to Progress in Oceanography June 2006

Key Words: Physical-Biological Modeling, Regime Shifts, Interdecadal Variability, Marine Ecosystems
Region Key Words: North Pacific, Gulf of Alaska

Corresponding Author:
Michael Alexander
NOAA, Earth System Research Laboratory
Physical Science Division
R/PSD1
325 Broadway
Boulder, CO 80305-3328
USA
Michael.Alexander@noaa.gov

Abstract

A basin-wide interdecadal change in both the physical state and the ecology of the North Pacific occurred near the end of 1976. Here we use a physical-ecosystem model to examine whether changes in the physical environment associated with the 1976-77 transition influenced the lower trophic levels of the food web and if so by what means. The physical component is an ocean general circulation model, while the biological component contains 10 compartments: 2 phytoplankton, 2 zooplankton, 3 nitrogen, 2 silicate and CO_2. The model is forced with observed atmospheric fields during 1960-1999. During spring, when the mean plankton biomass peaks in the model, there is a strong (~40%) reduction in plankton biomass after the 1976 transition over the central Gulf of Alaska (GOA). The epoch difference in plankton appears to be controlled by the mixed layer depth (MLD). The enhancement of Ekman pumping after 1976 causes the halocline to shoal, and thus the MLD could not penetrate as deep in the central GOA during winter. As a result, more phytoplankton remains in the euphotic zone and phytoplankton biomass began to increase earlier in spring during 1977-88 relative to 1970-76. Zooplankton populations also increases but then grazing pressure leads to a strong decrease in phytoplankton by April followed by a drop in zooplankton by May: essentially the mean seasonal cycle of plankton biomass is shifted earlier in the year. Finally, there is a rebound in plankton concentrations leading to an enhancement in zooplankton biomass by mid summer after 1976. Observations, which are only available during summer, also show an increase over the GOA, but the increase is much greater in nature than in the model.

1. Introduction

Studies conducted over the past 15 years have provided a growing body of evidence for decadal climate variability across the Pacific Basin (e.g. Trenberth, 1990, Graham 1994, Zhang et al., 1997, Deser et al., 2004). The most prominent mode of decadal variability in the North Pacific was termed the Pacific Decadal Oscillation (PDO) by Mantua et al. (1997) based on transitions between relatively stable states of the leading pattern of sea surface temperature (SST) anomalies around the years 1925, 1947, 1977 and perhaps 1998. The 1976-77 "regime shift" was especially pronounced with an increase in the strength of the atmospheric circulation over the North Pacific including a deeper Aleutian low, which drove basin-wide changes in ocean temperatures, currents and mixed layer depth (e.g. Miller et al., 1994, Trenberth & Hurrell, 1994, Polovina et al., 1995, Deser et al., 1996, 1999). These climatic changes had a pervasive effect on marine ecosystems from phytoplankton throughout the food web to the top trophic levels (Mantua et al., 1997, Hare & Mantua, 2000, Benson & Trites, 2002).

Many hypotheses have been proposed for Pacific decadal climate variability, including the PDO, which can be classified into three broad categories: extratropical (Latif & Barnett, 1994, 1996, Neelin & Weng, 1997); tropically forced (Graham et al., 1994, Newman et al., 2003, Deser et al., 2004); and those due to tropical-extratropical interactions (Gu & Philander, 1997, Kleeman et al., 1999, Vimont et al., 2002). While the mechanism(s) responsible for the PDO have yet to be fully resolved, the climate shifts appear to be more complex than reversals between two nearly opposite states (Benson & Trites, 2002). For example, Bond et al., (2003) examined the state of the North Pacific Ocean via the amplitudes of first and second leading patterns of SST variability as a

function of time. While the years 1970-1975 and 1978-1988 were dominated by the opposite phases of the leading pattern, the PDO, the amplitude of the PDO was relatively modest during most of the 1960s, and the 1989 transition was primarily from the first to the second leading pattern. Thus, the periods used to define epochs will clearly impact the impression of "regime transitions" in the physical and biological systems.

While the dynamics underlying Pacific decadal variability are unresolved, the changes in the physical state of the ocean clearly influence the primary and secondary production in the North Pacific. For example, total chlorophyll a, a proxy for phytoplankton biomass, nearly doubled in the central North Pacific from 1968 to 1985 (Venrick et. al., 1987). Brodeur & Ware (1992; BW from hereon), Brodeur et al. (1996) and Rand and Hinch (1998) examined vertical net tows over the northeast Pacific during summer (June 15 - Jul 31) and found they were sufficient to estimate zooplankton biomass (primarily copepods and other mesozooplankton) for the periods 1956-1959, 1960-1962 and 1980-89. The zooplankton biomass was relatively high in the central portion of the Gulf of Alaska (GOA) during the early periods, while in 1980-1989 the biomass was greatest along the edges of the Alaskan Gyre, including the North American coast and extending from the Queen Charlotte Islands southwestward along the transition zone between the Central and Alaskan Gyres. Overall, the zooplankton biomass over the northeast Pacific was roughly two times greater during the 1980s than during the 1956-59 or 1960-62. McFarlane & Beamish (1992) also found that the copepod biomass increased after the winter of 1976-77 in the Gulf of Alaska. However, Sugimoto & Tadokoro (1997) found a decrease in both phytoplankton and zooplankton biomass in the northeast Pacific during the summers of 1980-1994 relative to those in 1960-1975, but the data

were very limited in the earlier period and the results could be impacted by interannual variability, as the biomass was much greater in 1970 than in any other year.

Several physical/chemical factors may influence primary productivity in the Pacific on interannual to decadal time scales (as reviewed by Francis et al., 1998, Miller et al. 2004). In portions of the Pacific phytoplankton, growth can be limited by temperature, the abundance of nitrogen and other macronutrients, and by the lack of sunlight. However, the eastern subarctic Pacific is a high nitrate low chlorophyll (HNCL) region where micronutrients, especially iron, are believed to limit the growth of phytoplankton in late spring and summer (Martin & Fitzwater, 1988), while iron and the lack of sunlight may co-limit growth in winter (Maldanado et al., 1999). In contrast, several ecosystem modeling studies suggest that grazing by zooplankton regulates phytoplankton growth (Evans & Parslow, 1985, Frost, 1991), which may work in combination with the limited iron supply to prevent a spring bloom in the northeast Pacific (Frost, 1991, Fasham, 1995). Ocean currents can impact ecosystems by transporting heat, salt, nutrients and plankton. For example, the transport of warm and/or fresh surface waters into a region can enhance the static stability and decrease vertical mixing.

Vertical mixing, and the mixed layer depth (MLD) in particular, are critical in linking the physical/chemical and biological processes discussed above (e.g. Mann 1993, Steele & Henderson 1993, Gargett, 1997). If the mixed layer is too deep, phytoplankton will be transported beneath the euphotic zone limiting their growth, but if the MLD is too shallow not enough nutrients will be mixed into the surface layer from below to sustain photosynthesis. In addition, if the MLD is sufficiently shallow in late winter for photosynthesis to occur and the resulting phytoplankton biomass is adequate to sustain

zooplankton populations, then when the mixed layer shoals in spring, grazing by zooplankton can limit algal growth rates.

Several studies have emphasized the impact of changes in MLD during 1976-77 on the lower trophic levels of the North Pacific ecosystems (Venrick et al., 1987, Polovina et al., 1994). BW hypothesized that changes in wintertime MLD over the northeast Pacific could impact the micronutrient supply and/or change the rate of primary productivity and the efficiency of zooplankton grazing in spring. Polovina et al. (1995) indicated that shoaling of the mixed layer in winter post 1976-77 could significantly enhance productivity in the Gulf of Alaska by increasing the light available for photosynthesis based on MLD estimated from temperature profiles and a plankton population dynamics model. However, it is unclear whether there is sufficient variability in the late winter MLD in the northeast Pacific to impact primary and secondary production (McClain et al., 1996) and the MLD depends more on salinity than temperature in this region (Freeland et al., 1997).

While several studies have emphasized the role of wind stirring on mixed layer depth, buoyancy forcing, as determined by the heat and salt flux at the surface, the penetration of solar radiation into the ocean, and the density jump at the base of the mixed layer also regulate MLD (Alexander et al., 2000). Over the global oceans, the pycnocline, the vertical layer where the density increases rapidly with depth, can be regulated by both temperature and salinity. In the subarctic Pacific during winter, the mixed layer extends down to the strong salinity gradient, or halocline, located between depths of 100 m to 180 m (e.g. Freeland et al., 1997). Thus, low-frequency changes in the Ekman pumping in the Gulf of Alaska, which vertically displaces the halocline, can impact the wintertime MLD.

Indeed, after the mid-1970s, the pycnocline was shallower in the central part of the Gulf of Alaska and deeper in a broad band following the coast, primarily due to the local response to Ekman pumping, although propagating features due to mean advection and boundary waves also impacted the pycnocline along the coast (Cummins & Lagerloef, 2002, Capotondi et al., 2005).

Changes in the physical state of the North Pacific Ocean during the 1976 and their impact on the phytoplankton and zooplankton were simulated by Haigh et al. (2001) using a four-component ecosystem model, with compartments for nutrients, phytoplankton, zooplankton and detritus, embedded in a 10-level isopycnal OGCM. They performed simulations for the years 1952-1975 and 1977-1989, using the period *mean* atmospheric forcing. The model reproduced the observed increase in phytoplankton in the central Pacific in summer and a southward displacement of the subtropical chlorophyll front in all seasons post 1976. The model also indicated an increase zooplankton over the eastern subarctic Pacific in summer during the 1980s, but the increase (of ~25%) was much smaller than in BW. In addition, the years analyzed were not identical to those in BW, the model was tuned to reproduce the microzooplankton distribution, rather than the mesoscale and larger zooplankton samples used by BW, and the pattern of the change between the two epochs was somewhat different than observed, e.g. the zooplankton biomass decreased rather than increased along the coast of Alaska and Canada in the later period.

Chai et al. (2003) used an OGCM-ecosystem model, with time dependent forcing and substantially different physical and biological components than Haigh et al. (2001), to investigate decadal changes in the Pacific Ocean. Chai et al. focused on the subtropical

chlorophyll front, which expanded and extended further south after the 1976-77 shift, in agreement with Haigh et al. (2001). In the present study, we use the model simulation described by Chai et. al. to investigate the physical and biological changes during 1976-77 in the northeast Pacific Ocean, by comparing the simulated epoch differences to observations and then identifying the key physical and biological processes that cause the ecosystem changes.

2. The Model Simulation

The physical component of the model, which simulates temperature, salinity and currents, is the National Center for Atmospheric Research (NCAR) ocean model (NCOM), described by Large et al. (1997) and Gent et al. (1998). NCOM is derived from the Geophysical Fluid Dynamics Laboratory (GFDL) Modular Ocean Model with the addition of a mesoscale eddy flux parameterization along isopycnal surfaces (Gent & McWilliams 1990) and a non-local planetary boundary layer parameterization (Large et al., 1994). The advection of tracers, including temperature, salinity and the biochemical components, is calculated using a third-order differencing scheme. The background horizontal and vertical mixing coefficients for all tracers are 2.0×10^6 cm^{-2} $sec^{-1}$and 0.1 cm^{-2} sec^{-1}, respectively. The version of the model used here, described by Li et al. (2001), covers the Pacific from 45°S to 65°N and from 100°E to 70°W with realistic geometry and bathymetry. A sponge layer, where the model's temperature, salinity, nitrate and silicate are relaxed towards observations, is applied within 10° of the walls at 45°S to 65°N. The longitudinal resolution is a uniform 2°. The latitudinal resolution is 0.5° within 10° of the equator and increases to 2° poleward of 20° of the equator. There are 40

vertical levels, with 23 in the upper 400 m.

The biological model, developed by Chai et al. (2002), consists of ten compartments with two classes of phytoplankton (P1, P2) and zooplankton (Z1, Z2), two forms of dissolved inorganic nitrogen: nitrate (NO_3) and ammonium (NH_4), detrital nitrogen (DN), silicate ($Si(OH)_4$), detrital silicon (DSi), and CO_2 (Fig. 1). Small phytoplankton (P1) have variable growth rates, that depends on nitrogen and light. Their biomass is regulated by micrograzers (Z1), while their net productivity is largely remineralized (Landry et al. 1997). The large phytoplankton class (P2 > 10 μm) represents the diatom functional group, which can grow rapidly under optimal nutrient conditions (Coale et al., 1996). The micograzers have growth rates similar to P1 and density dependent grazing rates (Landry et al. 1997). The mesozooplankton (Z2) graze on P2 and DN and prey on Z1 and have a feeding threshold based on conventional grazing dynamics (Frost & Frazen, 1992). Sinking particulate organic matter is converted to inorganic nutrients via regeneration, similar to the process described by Chai et al. (1996). Nitrogen is the "currency" in the ecosystem model, i.e. plankton and detritus biomass are in units of millimoles of nitrogen per cubic meter (mmol N m^{-3}). A detailed discussion of the model equations and parameter values is given in Chai et al. (2002).

The model's temperature, salinity and nutrients were initialized using climatological values from the National Ocean Data Center (NODC), while the biological components were assigned a value of 0.025 mmol m^{-3} at the surface, decreasing exponentially with a scale length of 120 m – the average depth of the euphotic zone. The full model was then integrated for 10 years with climatological forcing, during which it reached a stable

annual cycle in the upper ocean. During this spin-up period and in the subsequent model experiment the physical and ecosystem components were integrated synchronously.

In the simulation examined here, the model is forced with observed atmospheric fields over the period 1955-1999 and monthly data are archived during 1960-1999, allowing for a five-year spin-up period. The surface fluxes of momentum, heat, fresh water, and insolation used to drive the model were derived from monthly mean values obtained from the Comprehensive Ocean Atmosphere Data Set (COADS; da Silva et al., 1994) over the period 1955-1993. From 1993-1999 the surface fluxes were obtained from the National Center for Environmental Prediction (NCEP) reanalysis (Kalnay et al., 1996, Kistler et al., 2001). The heat flux includes shortwave and longwave radiation and the sensible and latent heat flux. The model does not include the diurnal cycle, so the daily averaged insolation is used for calculating photosynthesis. The fresh water flux, given by precipitation minus evaporation, is used to drive the model. The surface salinity is also restored (using a 30-day time scale) towards the observed climatological monthly mean values obtained from Levitus et al. (1994), since precipitation is not well measured over the ocean. While this damping greatly reduces the surface salinity variability, the deeper ocean, including the halocline, is relatively unconstrained. More detailed descriptions of the procedures used to initialize and force the model are provided by Li et al. (2001) and Chai et al. (2003).

The model's fidelity in simulating the physical and biological state of the Pacific Ocean has been examined by Li et al. (2001) and Chai et al. (2003). While the model reproduces many aspects of the mean state and variability in the Pacific, it overestimates the phytoplankton biomass during late spring/early summer in the northeast Pacific, e.g.

the model's phytoplankton concentration is approximately twice that observed at Ocean Weathership P (50°N, 145°W) during April-June (Chai et al., 2003). This bias is likely due to the ecosystem model's inadequate treatment of micronutrients. While the model's implicit treatment of iron limitation via parameters that control the growth rate of diatoms maybe adequate for the equatorial Pacific (Chai et al., 2002), it appears to be unsuitable for the subarctic waters in the northeast Pacific. In addition, while the model's relatively coarse resolution allows us to examine basin-scale variability over an extended period of time, it is not sufficient to resolve coastal processes.

3. Results

3.1 Comparison with observations

To test the models ability to reproduce decadal variability, we compare epoch differences in the physical and biological state of the model to the available observations. We will mainly focus on the years 1970-76 and 1977-88 since they were dominated by opposite phases of the PDO (Bond et al., 2003) and because the fields used to force the model during these years were all derived from COADS (NCEP reanalysis is used to drive the model after 1993). The observed and simulated North Pacific sea surface temperature (°C) in 1977-1988 minus 1970-1976 (ΔSST) during February-March-April (FMA) are shown in Fig. 2. In both observations and the OGCM cold water in the central and western Pacific between approximately 25°N-45°N is ringed by warm water over the remainder of the North Pacific, indicative of a change to the positive phase of the PDO after 1976. The model also reproduces several of the finer-scale features of the ΔSST

field, with negative centers at 30°N, 155°W and 40°N, 175°E, and positive centers in the vicinity of the Alaskan Peninsula and Baja California. The latter is part of a broad swath the extends over much of the tropical Pacific suggesting that the PDO is part of a larger pattern that includes the tropics as well as the North Pacific, consistent with the findings of Zhang et al. (1997), Newman et al. (2003), Deser et al. (2004), and Schneider and Cornuelle (2005).

While the close correspondence between the observed and GCM ΔSST fields provides some confidence in the model's ability to simulate decadal changes, some discrepancies occur. For example, the large amplitude negative feature near 40°N, 145°E in the model does not occur in nature. In addition, by using the observed air temperature and model SST to compute the surface fluxes constrains the SSTs to track observations (see Seager et al., 1988, Alexander and Deser, 1995, Seager et al., 1995).

The difference in zooplankton biomass between the years 1960-1962 and 1980-1989, the periods when both observations and model output are available, is shown for the northeast Pacific in Fig. 3. The original observations used in BW were interpolated to the model grid by including all observations within a 200 km radius of a grid point and then inversely weighting the observed values based on their distance from that point. An exact model-data comparison is not possible as the observations are from vertical net tows (in gm /100 m^3) taken during June 15th-July 15th, while the model results (in mmol N/m^3) are based on monthly mean data in June and July for the two zooplankton classes integrated over the over the top 150 m. The general pattern of the difference between periods in the model resembles observations, in that there is an increase in biomass over most of the domain that is most pronounced around the rim of the Alaskan Gyre. While the minimum

values occur in the vicinity of 51°N, 152°W, they are slightly above zero in nature and below zero in the model. In addition, the magnitude of the epoch difference is much smaller in the model, which exhibits a ~5-10% increase over the GOA compared to a doubling in observations (BW). The number of observations, however, is limited, with 197 and 173 measurements over the domain in the 1960-62 and 1981-88 periods, respectively. Thus, unresolved spatial and temporal variability in nature, in addition to model biases and errors in the forcing fields, may contribute to the model-data differences seen in Fig. 3.

3.2 Physical – Biological linkages

A number of studies, including BW, Polovina et al. (1995) and Freeland et al. (1997), indicated that surface mixing in winter has a strong impact on the Gulf of Alaska ecosystem over the course of the seasonal cycle. The epoch difference (Δ, defined from hereon as 1977-1988 minus 1970-1976) in MLD (m) during FMA is shown for the GOA in Fig. 4. The MLD is defined as the depth where the potential density is 0.125 kg/m^3 greater than the surface value. The mixed layer shoals by more than 20 m in the central gulf in 1977-1988 relative to 1970-1976, a reduction in MLD by ~30%. Unlike in temperate waters where there is a robust inverse relationship between SST and MLD anomalies (e.g. see Deser et al., 1996), the shoaling in the central GOA (Fig. 4) occurs where there is little change in temperature (Fig. 2), while along the coast of North America the ΔSST and ΔMLD are both positive.

The MLD overlain on the temperature and salinity profiles in FMA averaged over a region in the central GOA (46°N-52°N, 160°W-140°W, box in Fig. 4) is shown in Fig. 5

from 1960 to 1999. The MLD, which extends to the upper portion of the halocline, closely tracks the vertical variations in salinity but not temperature, including the epoch changes in the halocline around 1976. The close correspondence between MLD and the halocline occurs even though the salinity variations near the surface are negligible in the model due to the strong restoring of the surface salinity towards climatology. Furthermore, the epoch difference in salinity, at depths of 70 m to 150 m, closely resembles the MLD pattern, with increased salinity in the center of the gyre and decreased salinity along the coast (not shown). Our results, in conjunction with those of Freeland et al. (1997) and Capotondi et al. (2005), indicate that the wintertime MLD in the GOA is primarily set by dynamical ocean processes that regulate the depth of the halocline (which determines the pynocline) and not by changes in the surface wind mixing, buoyancy forcing or fresh water flux. The shoaling of the halocline and hence the mixed layer in the central GOA, reflects the enhanced Ekman pumping associated with a deeper Aleutian low and stronger circulation in the Alaskan gyre during 1977-88 relative to 1970-76 (not shown).

Changes in MLD influence primary productivity by regulating the amount of light and nutrients available for photosynthesis. In the northeast Pacific, the highest primary productivity integrated over the upper 100m of the model occurs in March-May (as discussed in section 3.3 and shown in Fig. 13). The epoch difference in primary productivity (ΔPP in mmol N m^{-2} day^{-1}) during MAM is shown in Fig. 6. The ΔPP pattern, with a decrease in the central GOA ringed by an increase along the coast, is remarkably similar to the structure of ΔMLD (Fig. 4); indeed the pattern correlation between the two is 0.91. Given that where the MLD is shallower the productivity is

reduced, and vice versa, suggests that the vertical mixing of nutrients into the surface layer, rather than light limitation, may be the cause of the simulated biological changes following 1976 in the GOA.

The nitrate ($N0_3$) and dissolved silica (H_4SiO_4) concentrations (mmol m^{-3}) during MAM are shown for the average over the 1977-1988 period (contours) and for 1977-1988 minus 1970-76 (shading) in Fig. 7. Nitrate is an essential nutrient for both phytoplankton groups, while silica is an important structural element for diatoms, represented by the large phytoplankton group. There is a small reduction in both nitrate and silica in the central GOA after 1976, where the decrease in $N0_3$ at 50°N, 145°W (the location of ocean weather station P) is consistent with the findings of Freeland et al. (1997). However, the ΔNO_3 and ΔH_4SiO_4 is a small fraction (< 10%) of the mean concentration of nutrients during 1977-1988. The pattern of the epoch shift in the nutrient concentrations is also quite different than the change in primary productivity, e.g. the greatest decrease in primary productivity occurs in the vicinity of 46ºN, 150ºW (Fig. 6), where both NO_3 and H_4SiO_4 strongly increase (Fig. 7). Finally, the concentrations of both NO_3 and H_4SiO_4 exceed 5 mmol m^{-3} over most of the northeast Pacific during 1977-1988, sufficient to maintain rapid phytoplankton growth. Indeed, in the GOA region the NO_3 and H_4SiO_4 concentrations could sustain ~90% of the maximum growth rate as indicated by the nutrient regulation functions for P1 and P2 in the ecosystem model (Chai et al., 2002).

3.3 MLD, Light Limitation and Trophic Interactions

What is the primary factor linking the epoch difference in MLD with primary productivity in the GOA if it is not a change in (macro) nutrients? One possibility is changes in micronutrients, especially iron. However, iron is not directly included in the model and its indirect impact is limited in high latitudes (see Chai et al., 2003). An alternate hypothesis is that changes in MLD *do* impact phytoplankton via altering the light available for photosynthesis, but then trophic interactions modify the initial biological response as the seasonal cycle progresses. Specifically, a shoaling of the wintertime MLD in 1977-88 relative to 1970-76 leads to more light and thus enhanced primary productivity and greater phytoplankton biomass earlier in the year in the central GOA region. The resulting increase in phytoplankton enhances the food supply enabling a more rapid rise in the zooplankton biomass, but the associated increase in grazing subsequently suppresses phytoplankton and then zooplankton biomass during their peak in spring. Finally, the reduction in zooplankton during spring may lead to a weak rebound in plankton biomass by summer.

As a first step in testing this hypothesis we examine if the epoch changes are coherent across trophic levels and then if these changes fluctuate over the seasonal cycle. The 1977-88 mean and Δ in biomass are shown in Fig. 8a-d for each of the four plankton classes over the northeast Pacific. (The mean values during 1977-88 are similar to those from the entire 1960-1999 record - not shown). The biomass values (N mmol m^{-3}) are presented during the calendar month in which the mean and Δ peak: March for small phytoplankton (P1), April for micro zooplankton (Z1) and large phytoplankton (P2), and May for meso zooplankton (Z2). The biomass shown in Fig. 8 (and from hereon) is obtained from the surface layer (0-10 m) of the model. The mean P1 and P2 biomass

(contours) peaks at ~50°N, while the Z1 and Z2 reach maximum values north of ~52°N. The Δ biomass for all four plankton classes (shaded) is negative and of large amplitude relative to the mean, indicating a substantial decrease in biomass after 1976. For example, P2 decreases by more than 60% in the vicinity of 46°N, 150°W during April. The reduction in both phytoplankton and zooplankton biomass are collocated and centered within and slightly to the south of the maximum in the long-term mean.

The average biomass in the two periods and the difference between them are presented as a function of calendar month for the central GOA region in Fig. 8e and 8f, respectively. The ~40% decrease in P and Z biomass in the central GOA region during its peak in 1977-1988 relative to 1970-76 is both preceded and followed by an increase in biomass in all four plankton classes, although the increase is relatively small except for P2 and Z2 in March and April, respectively. The spatial coherence of ΔP and ΔZ, and the reversal in sign of the Δ in biomass with month is consistent with our hypothesis that trophic interactions and their evolution over the seasonal cycle play an important role in modulating the low-frequency ecosystem variability.

Given that the magnitude of the mean and the epoch difference in biomass are much greater for the larger plankton classes (Fig. 8), we focus on the dynamics of P2 and Z2 from hereon. The time series of the P2 and Z2 biomass (mmol N m^{-3}) from 1960-1999 averaged over the central Gulf of Alaska region for the months of March, April and May, along with the MLD (m) in March, are shown in Fig. 9. The MLD is well above average during the early epoch, except for 1970 and well below average for later epoch, except for 1977, 1980 and 1982, which are near normal. There is an inverse relationship between MLD and P2 biomass (Fig. 10a) as reflected by a -0.67 correlation (significant at the 99%

level) between the two over the entire record. The phytoplankton biomass in March is below normal for all years between 1971 and 1976 but it is near normal and has much greater interannual variability during the 1977-88 period, which suggests that the deeper mixed layer during the first period has a greater impact on photosynthesis and phytoplankton biomass then the shallower mixed layer in the later period. The asymmetry in the relationship between MLD and P2 biomass is suggested by a scatter plot of the two variables averaged over the GOA region during March, where the phytoplankton is nearly independent of MLD for depths of less than ~65 m (Fig 10a), Perhaps when the MLD is less than a given depth, which is a function of the insolation and absorption in the water column, enough light is available to sustain phytoplankton growth and thus it is not a strongly limiting factor. The existence of a clear cutoff depth, however, is difficult to determine given the P2 variability unrelated to changes in MLD, i.e. the scatter in Fig 10a.

In early winter, including March, the phytoplankton and zooplankton biomass vary simultaneously (Fig. 9); in the GOA region the correlation between P2 and Z2 in March is 0.72 (although the lag correlation between P2 in Feb with Z2 in Mar, has a similar value of 0.69). While the Z2 biomass is generally low during March, it is nearly zero during 1970-76, and very low zooplankton abundance can be a critical factor in enabling rapid phytoplankton growth in spring (Evans & Parslow, 1985, Frost, 1991, Fasham, 1995; our Fig. 10c). Indeed, the P2 biomass switches from well below normal in March to well above normal in April during 1970-1976 (Fig. 9). The Z2 biomass remains anomalously low in April, reflecting the limited food supply in the previous month. Both P2 and Z2 exhibit large interannual variability rather than regime-like behavior after

1976. While the P2 biomass has decreased substantially over the entire record by May, the P2 values have again switched to being above average during 1970-1976 period. Following the increase in P2 biomass in April the Z2 biomass is above normal during the early 1970s. The lagged P-Z relationships exhibited during 1970-1976 in March through May are also very robust over the entire 40-year record, as indicated by the limited scatter between P2 and Z2 (Fig. 10b,c), where the correlation between P2 in Mar (Apr) and Z2 in Apr (May) is 0.89 (0.95), and the correlation between Z2 in Mar (Apr) with P2 in Apr (May) is -0.84 (-0.85). The relationship between P2 with Z2 in the following month appears to be linear (Fig. 10b), with a greater change in Z2(Apr) relative to a unit change in P2(Mar) than for Z2(May) relative to P2(Apr). While a linear relationship provides a reasonable fit for Z2(Mar)-P2(Apr) and for Z2(Apr)-P2(May), the two combined suggest an inverse exponential relationship (Fig. 10c). The concurrent P2-Z2 correlations in the GOA region are -0.72 and 0.77 in April and May respectively; while significant the change of sign between months and the slight decrease in magnitude compared to the lag correlations, suggest that the concurrent P-Z correlation values during spring reflect the lag relationship between the two trophic levels. However, we may not be fully resolving the period of the lag with monthly data.

The timing of the mixed layer depth and plankton changes with respect to the seasonal cycle are examined further in Fig. 11 using time-latitude (Hovmöller) diagrams of monthly mean (contours) and Δ (shaded) values of MLD (m) and P2 and Z2 biomass (mmol N m^{-3}). The variables are averaged over 160ºW-140ºW and presented for 40°N-57°N from January through July. The maximum mean MLD exceeds 80 m during January-March in the vicinity of 50°N and then decreases at all latitudes to about 20 m by

May. The mean P2 biomass begins increasing in early winter, reaching a maximum in February, March, and April, for the latitude bands 40°-44°N, 44°-47°N and 48°-57°N, respectively, and then decreases rapidly in May. In addition to the seasonal cycle in insolation, the canonical evolution of P2 also depends on MLD, which is shallower in the southern part of the domain in JFM and thus more conducive for photosynthesis in a light-limited regime. The mean Z2 biomass increases during late winter, peaks in April-May and then declines but much more slowly than P2.

During January-March the Δ P2 biomass increases where the Δ MLD has decreased and vice versa, with the greatest increase in P2, located at 48°N in March, occurring in conjunction with the greatest decrease in MLD (shading, Fig. 11). This inverse relationship between ΔMLD and ΔP2, occurs over most of the domain during winter and is consistent with changes in light limitation influencing phytoplankton growth on decadal timescales. However, the relationship breaks down later in the spring and south of ~46°N in late winter as light is less of a factor in regulating primary productivity and grazing by zooplankton may have already begun to constrain the phytoplankton biomass.

As in the central GOA region, ΔP2 and ΔZ2 are enhanced prior to the annual mean peak in winter, reduced during and slightly after the peak in spring, and then weakly enhanced by summer between 40°N and 52°N (Fig. 11). In March-May, when the largest epoch differences in biomass occur, ΔP tends to lead ΔZ by one month (Figs. 8f, 9, 11b,c). For example, at 48°N the sharp increase in P2 in March is followed by a rapid rise in Z2 in April, while the decrease in P2 in April is followed by a decrease of Z2 in May. Likewise, the epoch changes in zooplankton tend to be inversely related to the

phytoplankton changes when the former leads by one month, e.g. positive ΔZ2 values at 46°N in March are followed by negative ΔP2 values in April.

To quantify the phytoplankton-zooplankton interactions, the following one-month lag correlations are presented in Fig. 12: a) P2 in March with Z2 in April; b) P2 in April with Z2 in May; c) Z2 in March with P2 in April and d) Z2 in April with P2 in May. The correlations are calculated locally at gridpoints in the northeast Pacific based on the entire 1960-99 record. The magnitude of the correlations exceeds 0.4 (significant at the 95% level) over most of the domain and 0.6 (significant at the 99% level) in the central GOA. The P2-Z2 correlations are positive and the Z2-P2 correlations negative for both March to April and April to May, which suggests that greater abundance of phytoplankton through enhanced primary productivity enables greater zooplankton growth in the following month, while more zooplankton suppress the phytoplankton population via grazing in the subsequent month.

Primary productivity of P2 and grazing of P2 by Z2 (mmol N m^{-2} day^{-1}) averaged over the upper 100 m are shown for northeast Pacific during the months of February through May in Fig. 13. The maximum primary productivity averaged over the 1977-88 period migrates from the southern to the northern edge of the GOA from February to May, as the amount of light necessary for photosynthesis moves northwards. This migration is not zonally uniform as the largest values occur in the latitude bands 135°W-140°W, 130°W-135°W and 135°W-150°W in Feb, Mar and Apr-May, respectively. The secondary maxima located along 40°N in May is associated with the poleward edge of the subtropical chlorophyll front, which extends into the northeast Pacific in late spring and summer. The overall maximum mean primary productivity occurs in April rather

than June (not shown), suggesting that factors other then the availability of light is limiting phytoplankton growth in late spring and summer. In general, the mean primary productivity and grazing patterns are very similar, although the latter is shifted south of the former but only by ~2º latitude. The collocation of the primary productivity and grazing is consistent with local grazing on P2 by Z2, since the plankton life cycles occur much faster than the advection by ocean currents. The slight southward displacement of grazing relative to primary productivity is likely due to the initiation of photosynthesis earlier in the seasonal cycle and thus further north relative to grazing by zooplankton.

Like the mean values, the epoch difference in primary productivity and grazing rates also move northward across the GOA from February to May and the grazing is shifted slightly south relative to the primary productivity (Fig. 13). The ΔPP and grazing rates are generally positive to the north and negative to the south of their respective maximum in the 1977-88 mean values, indicating a northward displacement in biological activity after the 1976 regime shift. The epoch differences are also a substantial fraction of the mean, e.g. primary productivity decreased by as much as ~70% in 1977-1988 relative to 1970-1976. There is generally a close correspondence between the epoch changes in the primary productivity and grazing rates for each calendar month. Thus there is both enhanced PP and grazing over much of the Alaskan gyre during February through April after 1976. The increase in grazing is especially pronounced between 48°N-52°N and 145°W-155°W in March and April; and likely contributes to the strong suppression of primary productivity in May in the central GOA. The seasonal evolutions of P2 and Z2 (not shown) are very similar to the corresponding patterns of PP and grazing shown in Fig. 13.

4. Summary and Conclusions

We have used a physical-ecosystem model to examine whether changes in the physical environment associated with the 1976-77 transition influenced the lower trophic levels of the food web and if so by what means. The model indicates higher zooplankton biomass in the northeast Pacific during summer in 1977-88 relative to 1960-62 as occurred in nature and the pattern of the change was similar to nature with enhanced biomass around the periphery of the gyre. Observations, however, suggest that the biomass more than doubled over the GOA (BW), while the model indicates only about a 10% increase in biomass. The simulated epoch differences were much larger in spring, when the mean plankton biomass peaks in the model. In contrast to summer, there was a strong (~40%) reduction in plankton biomass after the 1976 transition over a region in the central GOA and as much as a 60% decrease in primary productivity in some grid squares during April. The epoch difference in spring primary productivity appears to be controlled by the winter mixed layer depth as the pattern correlation between the two is > 0.9. A positive correlation was unexpected since MLD and primary productivity should be inversely related in a light limited regime, as is believed to be the case in the northeast Pacific during winter and spring. However, we found that the phytoplankton growth was not nutrient limited, which led us to seek an alternate explanation for the epoch changes in northeast Pacific.

We hypothesize the following chain of events lead to the difference in the climate and biology in the central Gulf of Alaska in 1977-88 relative to 1970-76: The Aleutian Low was stronger (e.g. Trenberth & Hurrell, 1994), and the associated cyclonic winds

accelerated the Alaskan gyre and enhanced Ekman pumping (Capotondi et al., 2005). The associated increased upwelling caused the halocline to shoal. Thus the mixed layer, which extends to the upper portion of the halocline in winter, did not penetrate as deep. As a result, more phytoplankton remained in the euphotic zone and primary productivity and phytoplankton biomass increased earlier in spring. The enhanced food supply led to an increase in zooplankton biomass but then grazing pressure lead to a strong decrease in phytoplankton by April followed by a drop off in zooplankton by May. The one-month lag between P and Z likely reflects the timescales set by photosynthesis and grazing, although this was based on monthly averaged data and does not consider all of the potential biological interactions in the system such as nutrient recycling (see Fig. 1). Finally, there was a weak rebound in plankton concentrations by mid summer after 1976. This hypothesis should be evaluated further using observations, additional model simulations, preferably with higher temporal resolution data to better resolve the seasonal evolution of the epoch differences and stand alone simulations to test the sensitivity of the ecosystem to changes in MLD and trophic interactions.

As in previous studies the winter mixed layer depth appears to be a critical variable for ecosystem dynamics in the North Pacific. Decadal variability of MLD in the northeast Pacific appears to depend on dynamical ocean process that influence the density jump at the base of the mixed layer (and top of the halocline), rather than the local wind-induced mixing. Interannual and decadal changes in MLD and phytoplankton biomass in the GOA are inversely related, indicative of a light limited ecosystem as suggested by (Boyd et al., 1995, Polovina et al., 1995), but *only* during winter. Subsequent changes in grazing rates appear to cause larger changes in biomass during their spring peak, leading to a

positive correlation between winter MLD and spring primary productivity/plankton biomass. The importance of grazing in regulating the spring plankton biomass in the northeast Pacific has been noted before using one-dimensional ecosystem models in the context of the mean seasonal cycle (Evans and Parslow, 1985, Frost 1991, Fasham, 1995). The epoch differences in biomass can also be viewed as changes in the seasonal cycle with the spring transition, or alternatively the northward seasonal advance of primary and secondary production, beginning earlier in the year in 1977-88 relative to 1970-76. Stabeno and Overland (2001) and Bograd et al. (2002) have also found that decadal variability in the North Pacific climate and ecosystems can be manifest in the seasonal cycle.

Based on previous analyses (e.g. Bond et al., 2003) and the simulation of SST in the OGCM, we selected 1970-76 and 1977-88 as periods that exhibited "regime-like" behavior, i.e. when anomalies are of one sign. This appeared to be a fairly reasonable assumption for MLD depth, which is shallow (deep) during 1977-88 (1970-76) in the central GOA. However, the biological variables were only coherent during 1970-76; during 1977-88 phytoplankton and zooplankton biomass were close to their long-term means and exhibited substantial interannual variability. The reason for this difference between periods is unclear, although it may be due to a nonlinear relationship between MLD and primary productivity, i.e. the phytoplankton is much more sensitive to changes in MLD, when the latter exceeds ~65 m in the GOA region. Perhaps when the MLD is less than a given depth enough light is available to sustain phytoplankton growth and it is thus not a strongly limiting factor. The high degree of interannual variability during the later period also has important implications for assessing regimes based on observations:

insufficient sampling could lead to inaccurate estimates of the actual mean value over that period.

The model used in the present study may not adequately represent several potentially important processes, including the direct simulation of iron and its influence on primary productivity; eddies and coastal processes, such as Kelvin waves; and two-way interactions between zooplankton and higher trophic levels. The role of these processes on decadal variability of the physical and biological state of the north Pacific warrants further exploration.

Acknowledgements

We thank James Scott for his assistance in processing the data and drafting the figures and Yi Chao and collaborators for developing the OGCM and sharing the output with us. This research received financial support from the NOAA office of Polar Programs and NASA's IDS program.

References

Alexander, M.A., & Deser. C. (1995). A mechanism for the recurrence of wintertime midlatitude SST anomalies. *Journal of Physical Oceanography*, 25, 122-137.

Alexander, M.A., Scott, J.D. & Deser, C. (2000). Processes that influence sea surface temperature and ocean mixed layer depth variability in a coupled model. *Journal of Geophysical Research*, 105, 16,823-16,842.

Bond, N.A., Overland, J.E., Spillane, M., & Stabeno, P. (2003). Recent shifts in the state of the North Pacific. *Geophysical Research Letters,* 30, 2183.

Bograd, S., Schwing, F., Mendelssohn, R., & Green-Jessen, P. (2002). On the Changing Seasonality Over the North Pacific. *Geophysical Research Letters*, 29, doi:10.1029/2001GL013790.

Boyd P.W., Whitney F.A., Harrison P.J., et al. (1995). The NE subarctic Pacific in winter. 2. Biological rate processes. *Marine Ecology-Progress Series*, 128, 25-34.

Benson, A.J., & Trites, A.W. (2002). Ecological effects of regime shifts in the Bering Sea and eastern North Pacific Ocean. *Fish and Fisheries,* 3, 95-113.

Brodeur, R.D., & Ware, D.M. (1992). Long-term variability in zooplankton biomass in the subarctic Pacific Ocean. *Fisheries Oceanography*, 1, 32-38.

Brodeur, R.D., Frost, B.W., Hare, S.R., Francis, R.C., & Ingraham, W.J. (1996). Interannual variations in zooplankton biomass in the Gulf of Alaska and covariation with California Current zooplankton biomass. *CalCOFI Report*, 37, 80-99.

Capotondi, A., Alexander M.A., Deser, C. & Miller, A.J. (2005). Low-frequency pycnocline variability in the Northeast Pacific. *Journal of Physical Oceanography,* 35, 1403-1420.

Chai, F., Barber, R.T., & Lindley, S.T (1996). Origin and maintenance of high nutrient condition in the equatorial Pacific. *Deep-Sea Research II*, 42, 1031-1064.

Chai, F., Dugdale, R.C., Peng, T.-H., Wilkerson, F.P., & Barber, R.T. (2002). One-dimensional ecosystem model of the equatorial Pacific upwelling system. Part I: model development and silicon and nitrogen cycle, *Deep-Sea Research Pt II*, 49, 2713-2745.

Chai, F., Jiang, M., Barber, R.T., Dugdale, R.C., & Chao, Y. (2003). Interdecadal variation of the transition zone chlorophyll front: A physical-biological model simulation between 1960 and 1990. *Journal of Oceanography*, 59, 461-475.

Coale, K.H. et al. (1996). A massive phytoplankton bloom induced by an ecosystem-scale iron fertilization experiment in the equatorial Pacific Ocean. *Nature*, 838, 495-501.

Cummins, P.F. & Lagerloef, G.S. (2002). Low frequency pycnocline depth variability at station P in the northeast Pacific. *Journal of Physical Oceanography.* 32, 3207-3215.

Da Silva, A.M., Young-Molling. C.C, & Levitus, S. (1994). Atlas of Surface Marine Data: Vol. 1: Algorithms and Procedures. In *NOAA Atlas NESDIS 6*, p 83. U.S. Gov. Printing Office.

Deser, C., Alexander, M.A. & Timlin, M.S. (1996). Upper ocean thermal variations in the North Pacific during 1970 - 1991. *Journal of Climate*, 9, 1841-1855.

Deser, C., Alexander, M.A., & Timlin, M.S. (1999). Evidence for wind-driven intensification of the Kuroshio Current Extension from the 1970s to the 1980s. *Journal of Climate*, 12, 1697-706.

Deser C., Phillips, A.S., & Hurrell, J.W. (2004). Pacific interdecadal climate variability: linkages between the tropics and the North Pacific during boreal winter since 1900. *Journal of Climate*, 17, 3109–3124.

Evans, T.G., & Parslow, J.S. (1985). A model of annual plankton cycles. *Biological Oceanography,* 3, 327-347.

Fasham, M.J.R. (1995). Variations in the seasonal cycle of biological production in subarctic oceans: A model sensitivity analysis. *Deep-Sea Research,* 42, 1111-1149.

Freeland, H., Denman, K., Wong, C.S., Whitney, F. & Jacques, R. (1997). Evidence of change in the winter mixed layer in the Northeast Pacific Ocean. *Deep-Sea Research*, 44, 2117-2129.

Frost, B.W. (1991). The role of grazing in nutrient-rich areas of the open sea. *Limnology and Oceanography*, 36, 1616-1630.

Frost, B.W., & Frazen, N.C. (1992). Grazing and iron limitation in the phytoplankton stock and nutrient concentration: a chemostat analogue of the Pacific equatorial upwelling zone. *Marine Ecology Progress Series*, 83, 291-303.

Francis, R.C., Hare, S.R., Hollowed, A.B., & Wooster, W. S. (1998). Effects of interdecadal climate variability on the oceanic ecosystems of the NE Pacific. *Fisheries Oceanography*, 7, 1-21.

Gargett, A.E. (1997). The optimal stability 'window': a mechanism underlying decadal fluctuations in North Pacific salmon stocks? *Fisheries Oceanography*, 6, 109-117.

Gent, P.R. & McWilliams, J.C. (1990). Isopycnal mixing in ocean circulation models. *Journal of Physical Oceanography*, 20, 150-55.

Gent, P.R., Bryan, F.O., Danabasoglu, G., Doney, S., Holland, W.R., Large, W.G. & McWilliams, J.C. (1998). The NCAR Climate System Model Global Ocean Component. *Journal of Climate*, 11, 1287-306.

Graham, N.E. (1994). Decadal-scale climate variability in the tropical and North Pacific during the 1970s and 1980s: observations and model results. *Climate Dynamics*, 6, 135-162.

Graham, N.E., Barnett, T.P., Wilde, R., Ponater, M., & Schubert, S. (1994). On the roles of Tropical and mid-latitude SSTs in forcing interannual to interdecadal variability in the winter Northern Hemisphere circulation. *Journal of Climate*, 7, 1416-1441.

Gu, D. & Philander, S.G.H. (1997). Interdecadal climate fluctuations that depend on

exchanges between the tropics and extratropics. *Science*, 275, 805-07.

Haigh, S.P., Deman, K.L., & Hsieh, W.W. (2001). Simulation of the planktonic ecosystem response to pre- and post-1976 forcing in an isopycnic model of the North Pacific. *Journal of Fisheries and Aquatic Sciences*, 58, 703-722.

Hare, S.R., & Mantua, N.J. (2000) Empirical evidence for North Pacific regime shifts in 1977 and 1989. *Progress in Oceanography,* 47, 103-145.

Kalnay, E. & Coauthors. (1996). The NCEP/NCAR 40-year reanalysis project. *Bulletin of the American Meteorological Society*, 77, 437-71.

Kleeman, R., McCreary, J.P., & Klinger, B.A. (1999). A mechanism for the decadal variation of ENSO. *Geophysical Research Letters*, 26, 1743-1747.

Kistler, R., E. Kalnay, W. Collins, S. Saha, G. White, J. Woollen, M. Chelliah, W. Ebisuzaki, M. Canamitsu, V. Kousky, H. van den Dool, R. Jenne & Fiorinio, M. (2001) The NCEP-NCAR 50-year reanalysis: Monthly Means CD-ROM and documentation. *Bulletin of the American Meteorological Society*, 82, 247-67.

Landry, M R., Barber, R.T., Bidigare, R.R., Chai, F., Coale, K.H., Dam, H.G., Lewis, M.R., Lindley, S.T., McCarthy, J.J., Roman, M.R., Stoecker, D.K., Verity, P.G.. White, J.R. (1997). Iron and Grazing Constraints on Primary Production in the Central Equatorial Pacific: An EQPAC Synthesis. *Limnology and Oceanography*, 42, 8, 405-418.

Large, W.C., McWilliams, J.C. & Doney, S.C. (1994). Oceanic vertical mixing: a review and a model with a nonlocal boundary layer parameterization. *Reviews of Geophysics*, 32, 363-404.

Large, W. G., Danabasoglu, G., Doney S. C., & McWilliams, J. C. (1997). Sensitivity to surface forcing and boundary layer mixing in a global ocean model: Annual mean climatology. *Journal of Physical Oceanography*, 27, 2418-2447.

Latif, M. & Barnett, T.P. (1994) Causes of decadal climate variability over the North Pacific and North America. *Science*, 226, 634-637.

Latif, M. & Barnett, T.P. (1996). Decadal climate variability over the North Pacific and North America: dynamics and predictability. *Journal of Climate*, 9, 2407-2423.

Levitus, S., Burgett, R., & Boyer, T.P. (1994). NOAA Atlas NESDIS 4; World Ocean Atlas 1994 Volume 3: Salinity. In, Vol. 3. National Oceanic and Atmospheric Administration, Washington, D.C., U.S. Government Printing Office, 99 pp.

Li, X., Chao, Y., McWilliams, J.C., & Fu, L.-L (2001). A comparison of two vertical-mixing schemes in a Pacific Ocean general circulation model. *Journal of Physical Oceanography*, 14, 1377-1398.

Maldonado, M.T., Boyd, P.T., Harrison, P.J., and Price, N.P. (1999). Co-limitation of phytoplankton by light and Fe during winter in the subarctic Pacific Ocean. *Deep-Sea Research, II*, 46, 2475-2485.

Mann, K.H. (1993). Physical oceanography, food chains and fish stocks: a review. *ICES Journal of Marine Science*, 50, 105-119.

Mantua, N.J., Hare, S. R., Zhang, Y., Wallace, J.M., & Francis, R., (1997). A Pacific interdecadal climate oscillation with impacts on salmon production, *Bulletin of the American Meteorological Society*, *78*, 1069-1079.

Martin, J.H., & Fitzwater, S.E. (1988): Iron deficiency limits phytoplankton growth in the northeast Pacific subarctic. *Nature*, 331, 341-343.

McClain C.R., Arrigo, K. Tai, K.-S., Turk, D. (1996). Observations and simulations of physical and biological processes at ocean weather station P, 1951-1980. *Journal of Geophysical Research*, 101, 3697-3713.

McFarlane, G.A. & Beamish, R.J. (1992). Climatic influence linking copepod production with strong year-class in Sablefish, *Anoplopoma fimbria*. *Canadian Journal of Fisheries and Aquatic Sciences*, 49, 743-53.

Miller, A.J., Cayan, D.R., Barnett, T.P., Graham, N.E. & Oberhuber, J.M. (1994). Interdecadal variability of the Pacific Ocean: model response to observed heat flux and wind stress anomalies. *Climate Dynamics*, 10, 287-302.

Miller, A.J., Chai, F., Chiba, S., Moisan, J.R. & Neilson, D.J. (2004). Decadal-scale climate and ecosystem interactions in the North Pacific Ocean. *Journal of Oceanography*, 60, 163-188.

Neelin, J., & Weng, W. (1999). Analytical prototypes for ocean–atmosphere interaction at midlatitudes. Part I: coupled feedbacks as a Sea Surface Temperature dependent stochastic process. *Journal of Climate*, 12, 697-721.

Newman, M., Compo, G.P., & Alexander, M.A. (2003). ENSO-forced variability of the Pacific Decadal Oscillation. *Journal of Climate*, 16, 3853-3857.

Polovina, J.J., G. T. Mitchum, N. E. Graham, M. P. Craig, DeMartini, E.E. & Flint, E.N. (1994). Physical and biological consequences of a climate event in the central North Pacific. *Fisheries Oceanography*, 3, 15-21.

Polovina, J.J., Mitchum, G., & Evans, G.T. (1995). Decadal and basin scale variation in mixed layer depth and the impact on biological production in the central and North Pacific, 1960-1988. *Deep-Sea Research,* 42, 1701-1716.

Rand, P.S., & Hinch, S.G. (1998) Spatial patterns of zooplankton biomass in the northeast Pacific Ocean. *Marine Ecology Progress Series* 171, 181-186.

Schneider, N. & Cornuelle, B.D. (2005). The forcing of the Pacific Decadal Oscillation. *Journal of Climate*, 18, 4355-73.

Seager, R., Kushnir Y., & Cane, M. A. (1995). On heat flux boundary conditions for ocean models. *Journal of Physical Oceanography*, 25, 3219-3230.

Seager, R., Zebiak, S. E., & Cane, M. A. (1988). A Model of the Tropical Pacific sea-surface temperature climatology. *Journal of Geophysical Research-Oceans*. 93, 1265-1280.

Stabeno, P.J., & Overland, J. E. (2001). The Bering Sea shifts towards an earlier spring transition. *Eos Transactions, American Geophysical Union, 82*, 317-321.

Steele, J.H. & Henderson, E.W. (1993). The significance of interannual variability. In *Towards a model of ocean biogeochemical processes.* G.T. Evans & M.J.R. Fasham editors, NATO ASI series, Vol. 1, pp. 237-260.

Sugimoto, T. & Tadokoro, K. (1997). Interannual-interdecadal variations in zooplankton biomass, chlorophyll concentration and physical environment in the subartcic Pacific and Bering Sea. *Fisheries Oceanogaphy*, 6, 74-93.

Trenberth, K.E. (1990). Recent observed interdecadal climate changes in the Northern Hemisphere. *Bulletin of the American Meteorological Societ*y, 71, 988-993.

Trenberth, K.E. & Hurrell, J.W. (1994). Decadal atmosphere-ocean variations in the Pacific. *Climate Dynamics*, 9, 303-319.

Venrick, E.L., McGowan, J.A., Cayan, D.R., & Hayward, T.L. (1987). Climate and chlorophyll a: long-term trends in the Central North Pacific Ocean. *Science*, 238, 70-72.

Vimont, D.J., D. S. Battisti, & Hirst, A.C. (2002). Pacific interannual and interdecadal equatorial variability in a 100 year simulation of the CSIRO coupled general circulation model. *Journal of Climate*, 15, 160-78.

Zhang, Y., J. M. Wallace & Battisti, D.S. (1997). ENSO-like interdecadal variability. *Journal of Climate*, 10, 1004-1020.

Figure Captions

Fig. 1. Flow chart of the ecosystem model and its link to carbon and the physical model. The flow of nitrogen, silicon, carbon and heat through the system are indicated by white, red, orange and blue lines, respectively. Adapted from Chai et al. 2003.

Fig. 2. The epoch difference, 1977-88 – 1970-76 (Δ), in SST (°C) during January, February, March (JFM) from a) observations and b) the model simulation.

Fig. 3. The zooplankton biomass in 1980-1989 – 1960-1962, the years when both observations and model output are available. The observations, described by Brodeur and Ware (1992), were interpolated to the model grid by including all measurements within a 200 km radius of a grid point and then inversely weighting the observed values based on their distance from that point. The observations (gm /100 m^3) are from vertical net tows taken during June 15th-July 15th, while the model results (in mmol N m^{-3}) are based on monthly mean data in June and July for the two zooplankton classes integrated over the over the top 150 m. Grid squares without data are left blank.

Fig. 4. ΔMLD (m) during JFM. Values have been spatially smoothed using a 9-point filter. The box indicates the central Gulf of Alaska (GOA) region.

Fig. 5. The a) temperature (°C) and b) salinity (ppt) over the upper 120 m of the ocean during FMA in the central GOA region (46°N-52°N, 160°W-140°W) for the years 1960-1999. The MLD during February and FMA are shown by an open square and closed circle, respectively.

Fig. 6. As in Fig. 4, the Δ in primary productivity (PP in N m^{-2} day^{-1}) averaged over the upper 150 m of the ocean during JFM. The values have been spatially smoothed using a 9-point filter. The PP values can be converted from units of nitrogen to units of carbon by multiplying them by 6.625 as indicated by the Redfield ratio.

Fig. 7. The 1977-1988 mean (contours) and 1977-88 – 1970-76 (Δ, shading) for a) nitrate ($N0_3$) and b) dissolved silica (H_4SiO_4) concentrations (mmol m^{-3}) during MAM.

Fig. 8. As in Fig. 7, the 1977-88 mean (contours) and Δ (shading) for a) small phytoplankton (P1) in March, b) large phytoplankton (diatoms, P2) in April, c) microzooplankton (Z1) in April and d) mesozooplankton (Z2) in May. Also shown are the values of P1, P2, Z1, Z2 for each calendar month for the periods e) 1970-76 and 1977-88, and f) Δ, the difference between the two periods. The P and Z values (mmol N m^{-3}) presented here and the subsequent figures are from the top model level.

Fig. 9. The P2 and Z2 biomass (mmol N m^{-3}) from 1960-1999 averaged over the central Gulf of Alaska region for the months of a) March, b) April and c) May, along with the MLD (m, scale on right axis) in a) March. Also shown are the MLD, P2 and Z2 means (thin lines) over the 1960-1999 period.

Fig. 10. Scatter plot of a) MLD (March) with P2 (April), b) P2 (March) with Z2 (April) and P2 (April) with Z2 (May), c) Z2 (March) with P2 (April) and Z2 (April) with P2 (May). MLD (m) and P2 and Z2 (mmol N m^{-3}) values are for the central GOA region for the years 1960-99.

Fig. 11. Hovmöller (latitude-time) diagrams of the 1977-88 mean (contours) and Δ (shaded) values of a) MLD (m), b) P2 (mmol N m^{-3}) and c) Z2 (mmol N m^{-3}). The values are averaged over 160ºW-140ºW and shown for January through July.

Fig. 12. Correlations of a) P2 (March) with Z2 (April), b) P2 (April) with Z2 (May), c) Z2 (March) with P2 (April), and d) P2 (April) with Z2 (May). The Z2 are not present in the northeast GOA in March, hence correlations are not computed in this area, which is left blank in c).

Fig. 13. As in Fig. 7, the 1977-88 mean (contours) and Δ (shaded) P2 primary productivity (left column) and grazing of P2 by Z2 (right column) for the months of February, March, April, and May. The values have been averaged over the upper 150 m and are in units of mmol N m^{-2} day^{-1}.

Ecosystem Model

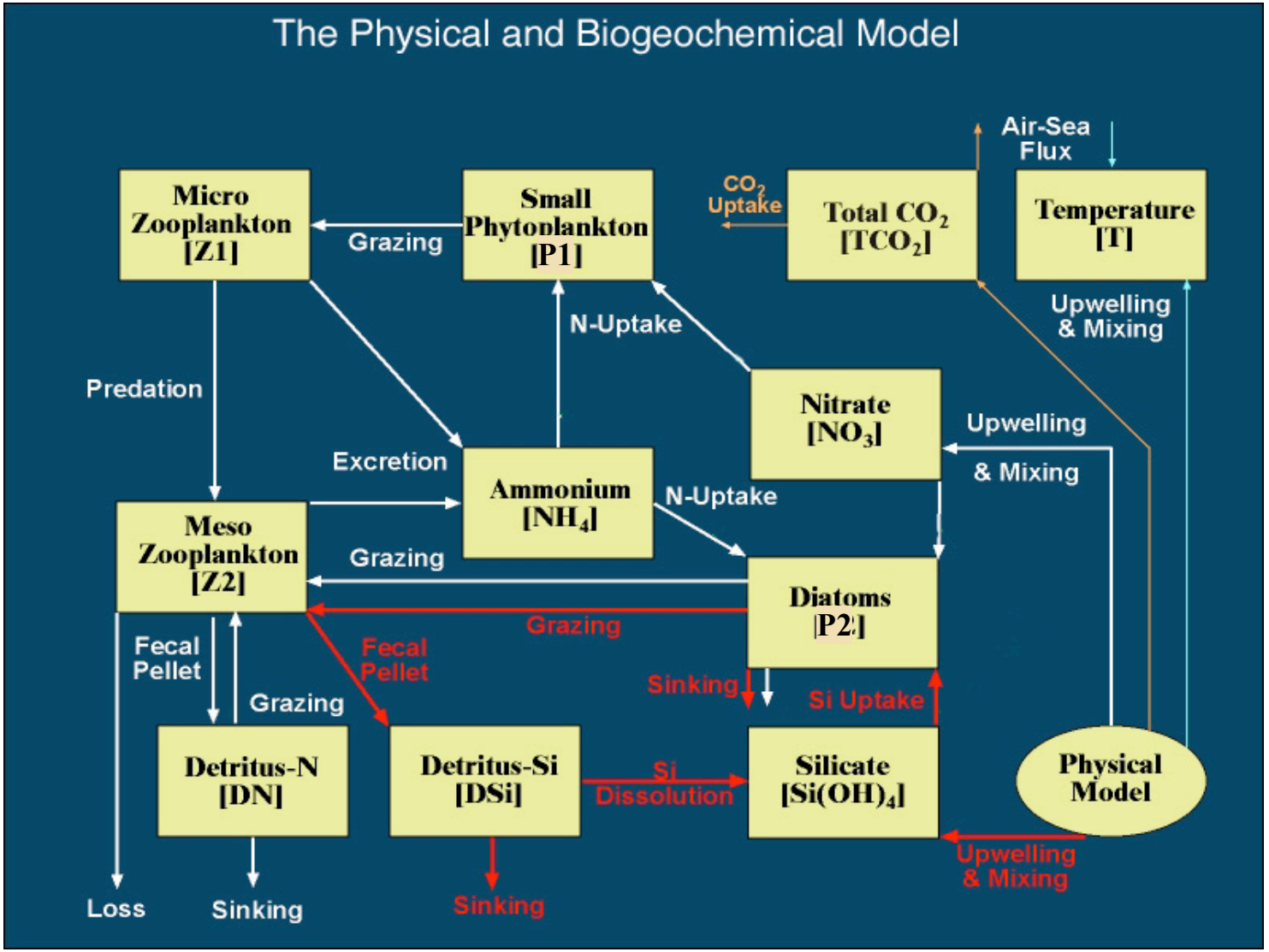

Fig 1. *From Chai et al. 2002; 2003*

SST(°C) 1977-88 – 1970-76 FMA

a) Observations

b) Ocean Model

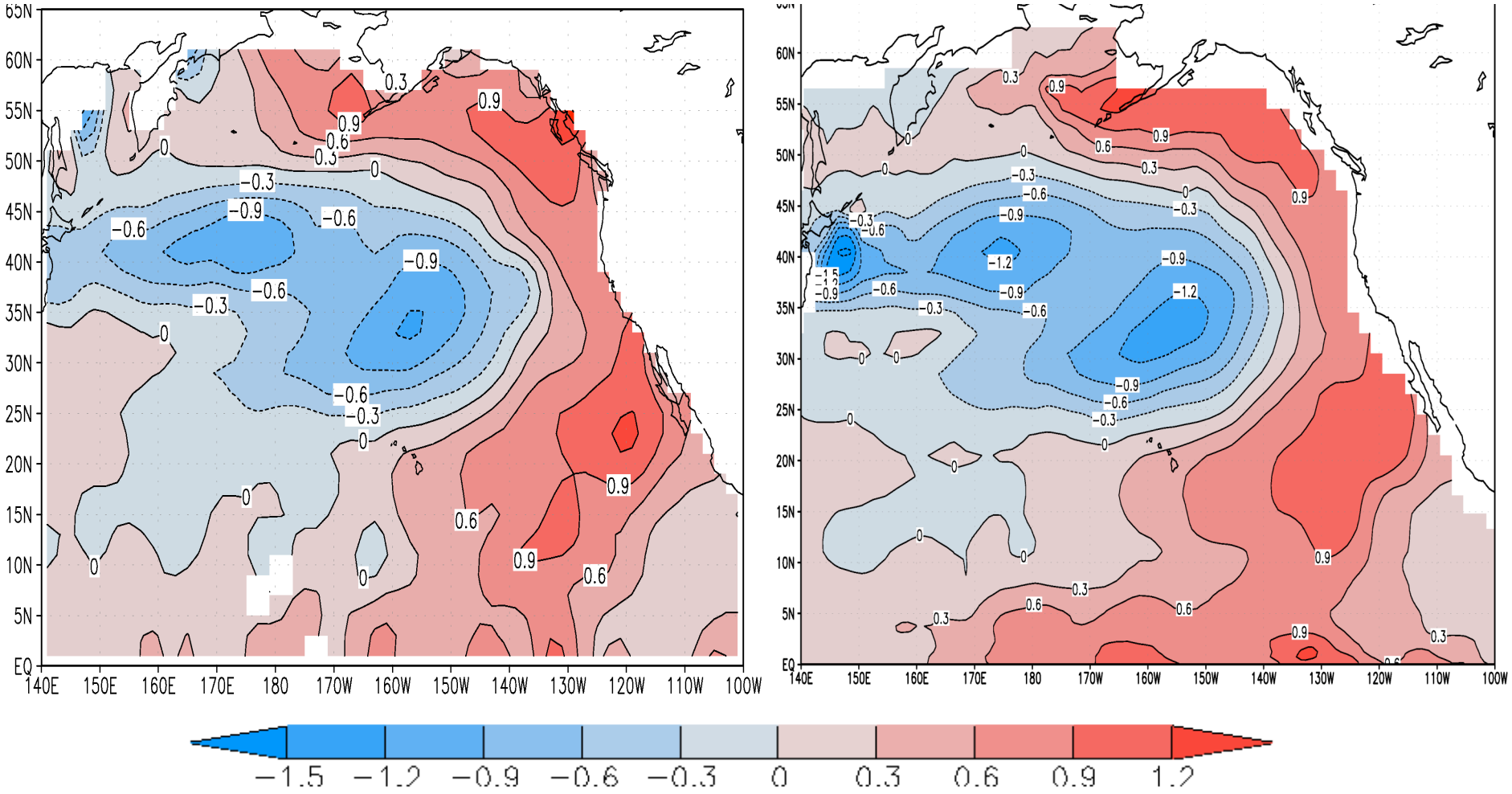

Fig. 2

Zooplankton 1980-89 – 1960-62

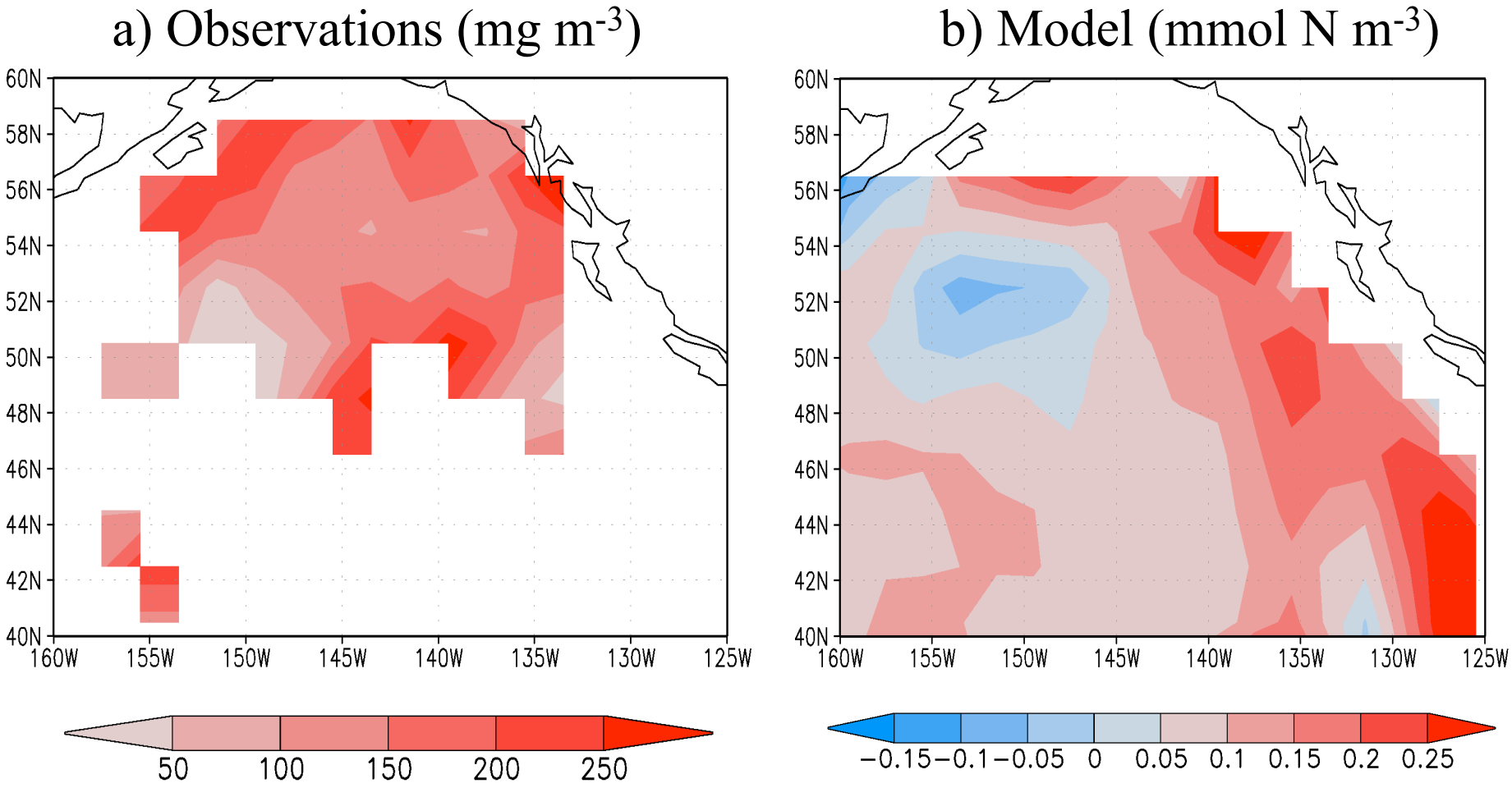

Fig. 3

Epoch Difference in MLD

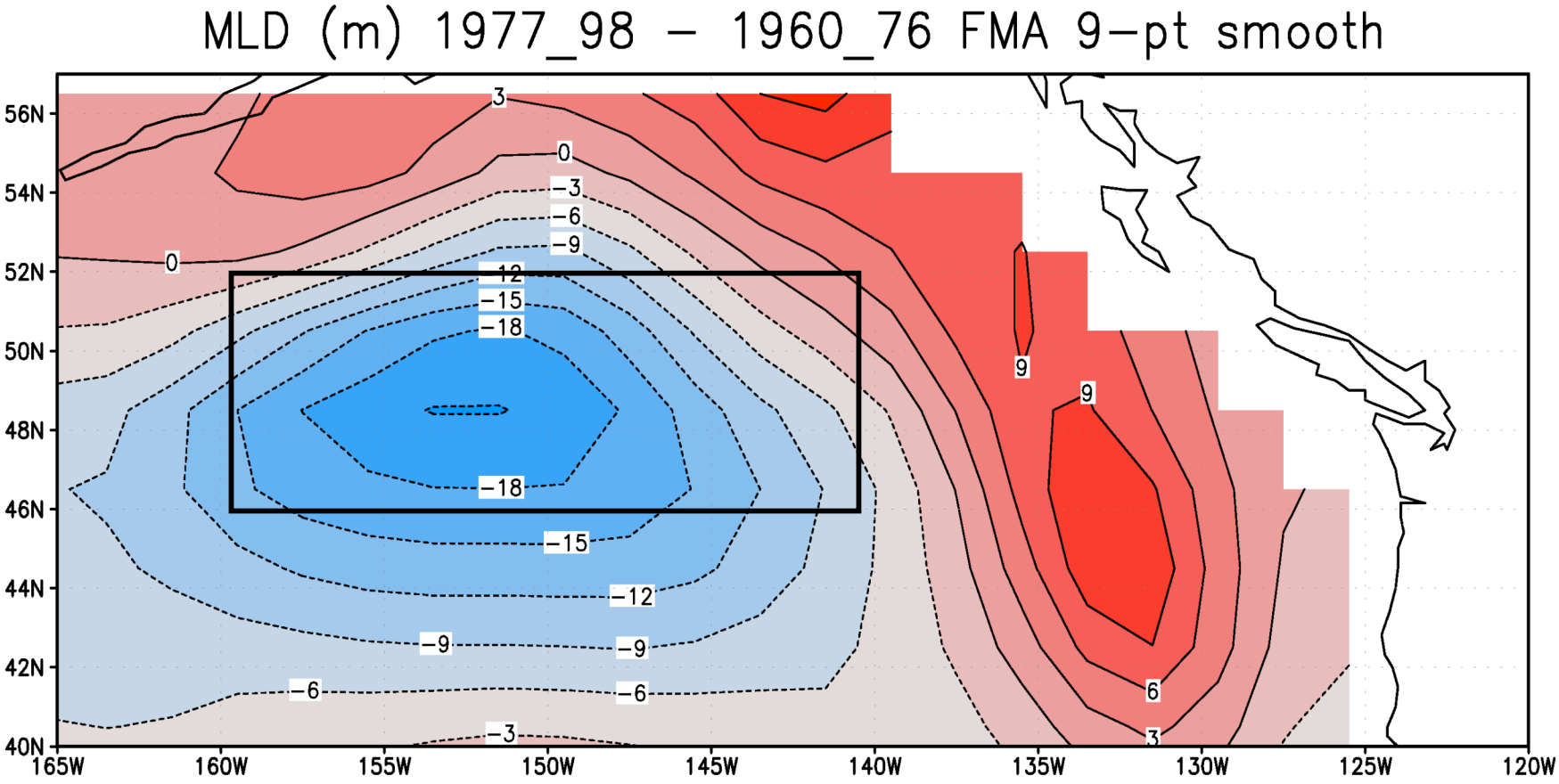

Fig. 4 MLD defined $\rho_z = \rho_{sfc} + 0.125$ kg m^{-3}
Box denotes central GOA region

MLD, Temperature, Salt in GOA Region

(46ºN-52ºN, 160ºW-140ºW) in FMA

Temperature (°C) and MLD

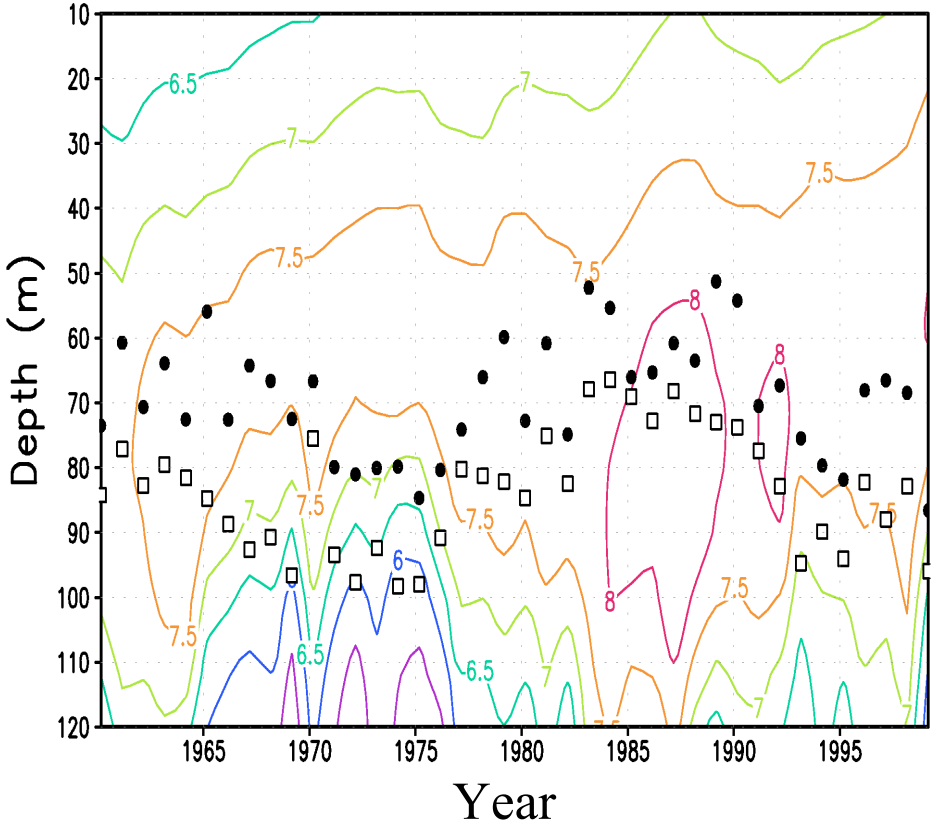

Salinity (ppt) and MLD

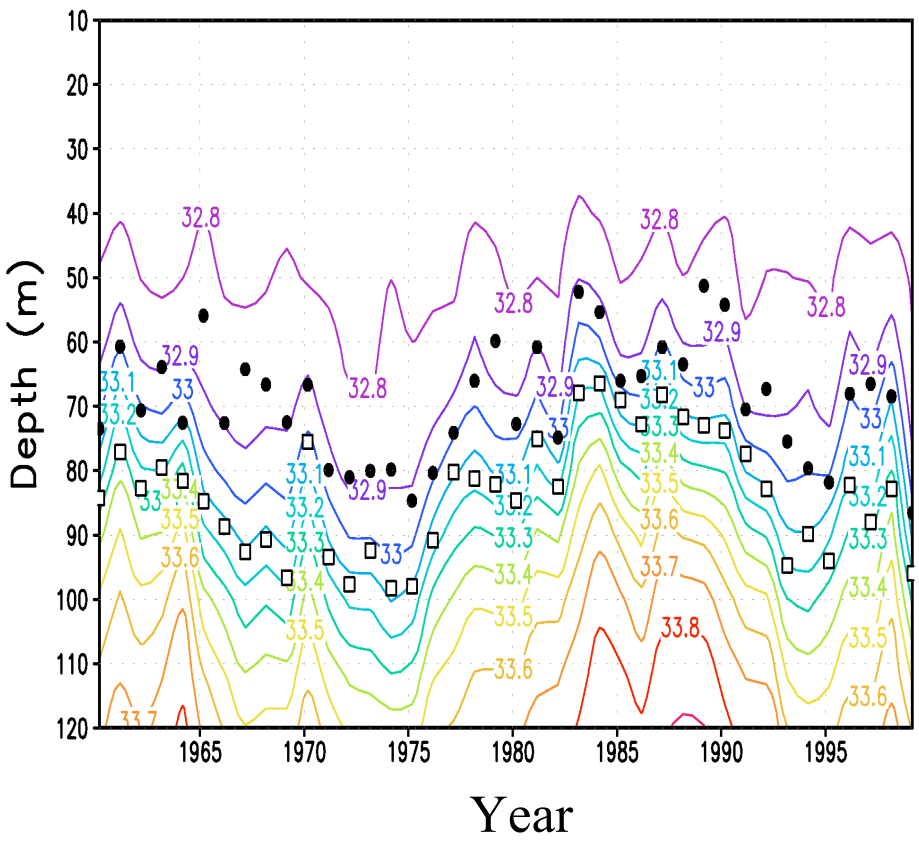

Fig. 5 □ MLD Feb ● MLD FMA

Primary Productivity (mmol of N m^{-2} day^{-1}) 1977-1988 - 1970-76 in MAM

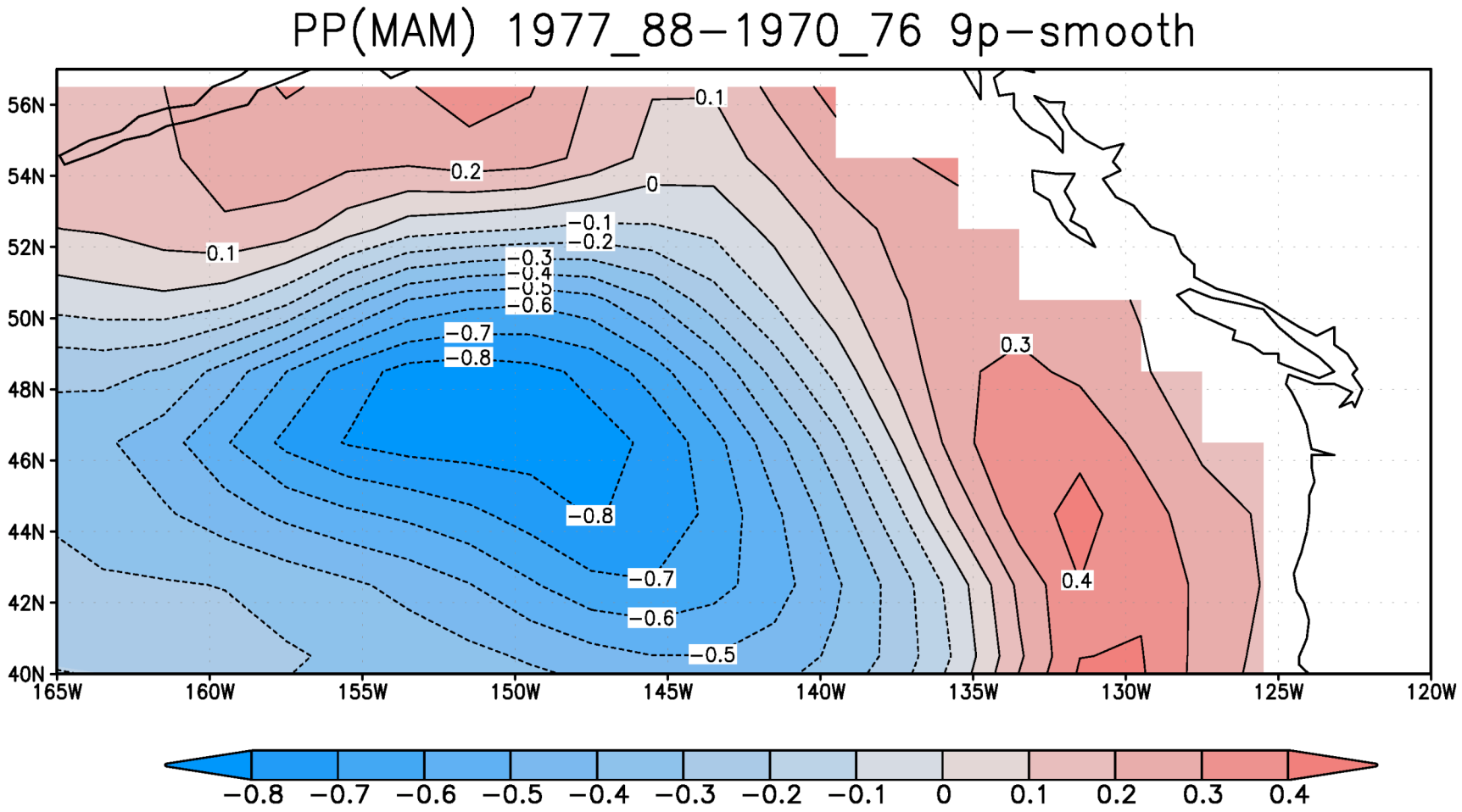

Fig. 6

Nutrients

1977-88 - 1970-76
(Shaded)

1977-88 average
(Contours)

MAM

Fig. 7

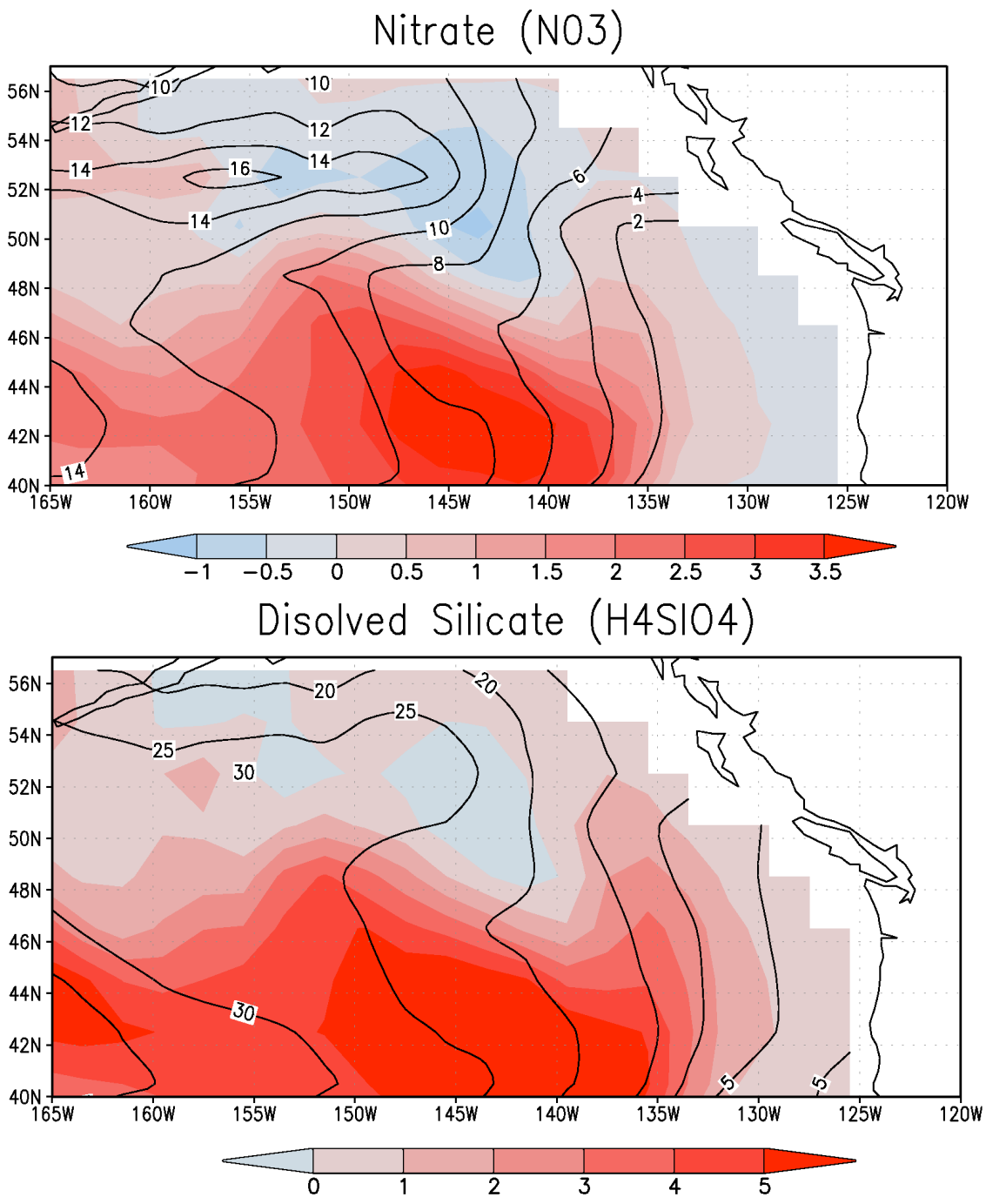

Plankton: 1977-88 - 1970-76 (shaded) 1977-1988 mean (contour)

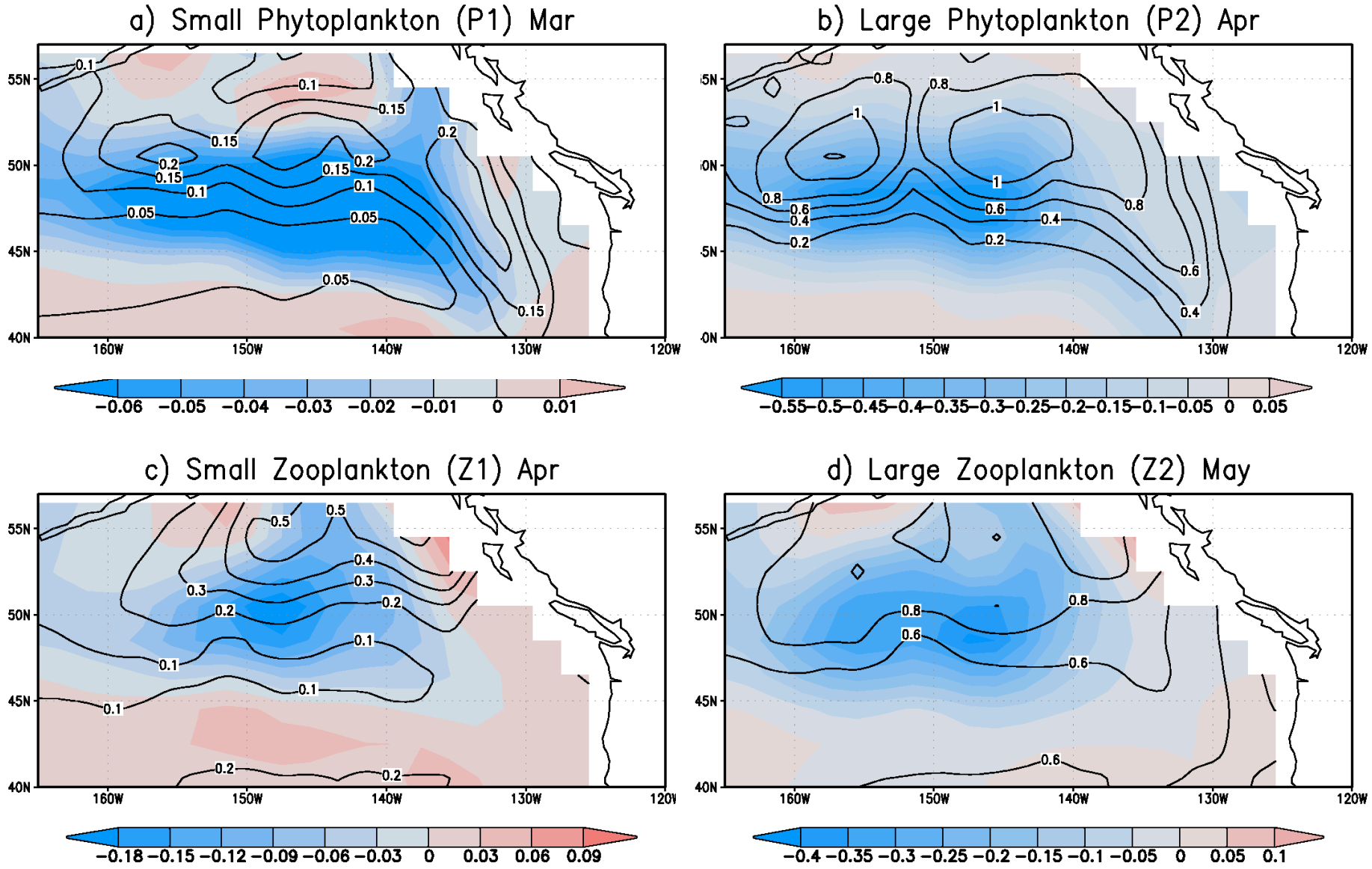

Fig. 8

Plankton Biomass (mmol N m^{-3})

Central/West GOA region: 46ºN-52ºN, 160ºW-140ºW

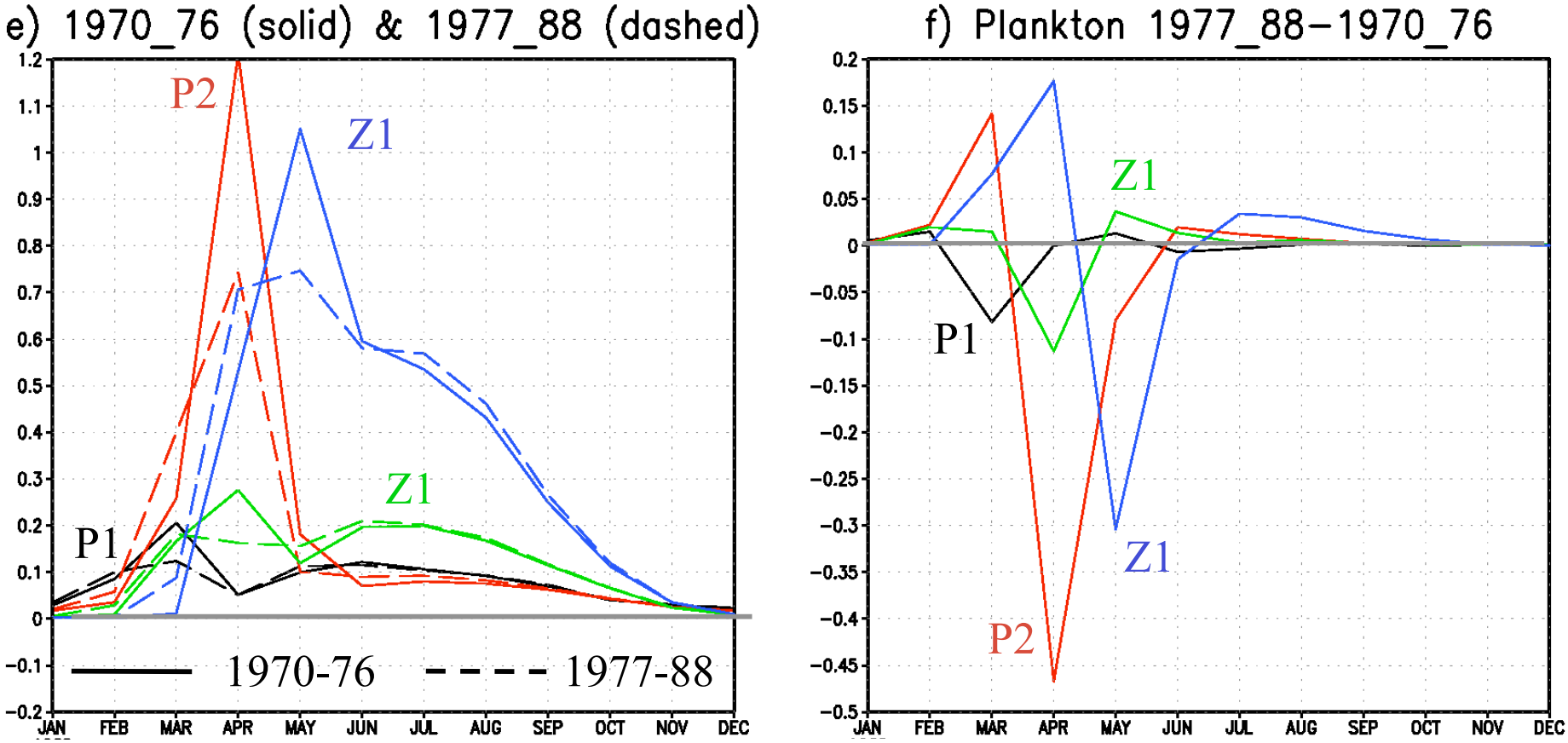

Fig. 8 (continued)

MLD (March) Plankton and Zooplankton Biomass in central GOA region

Fig. 9

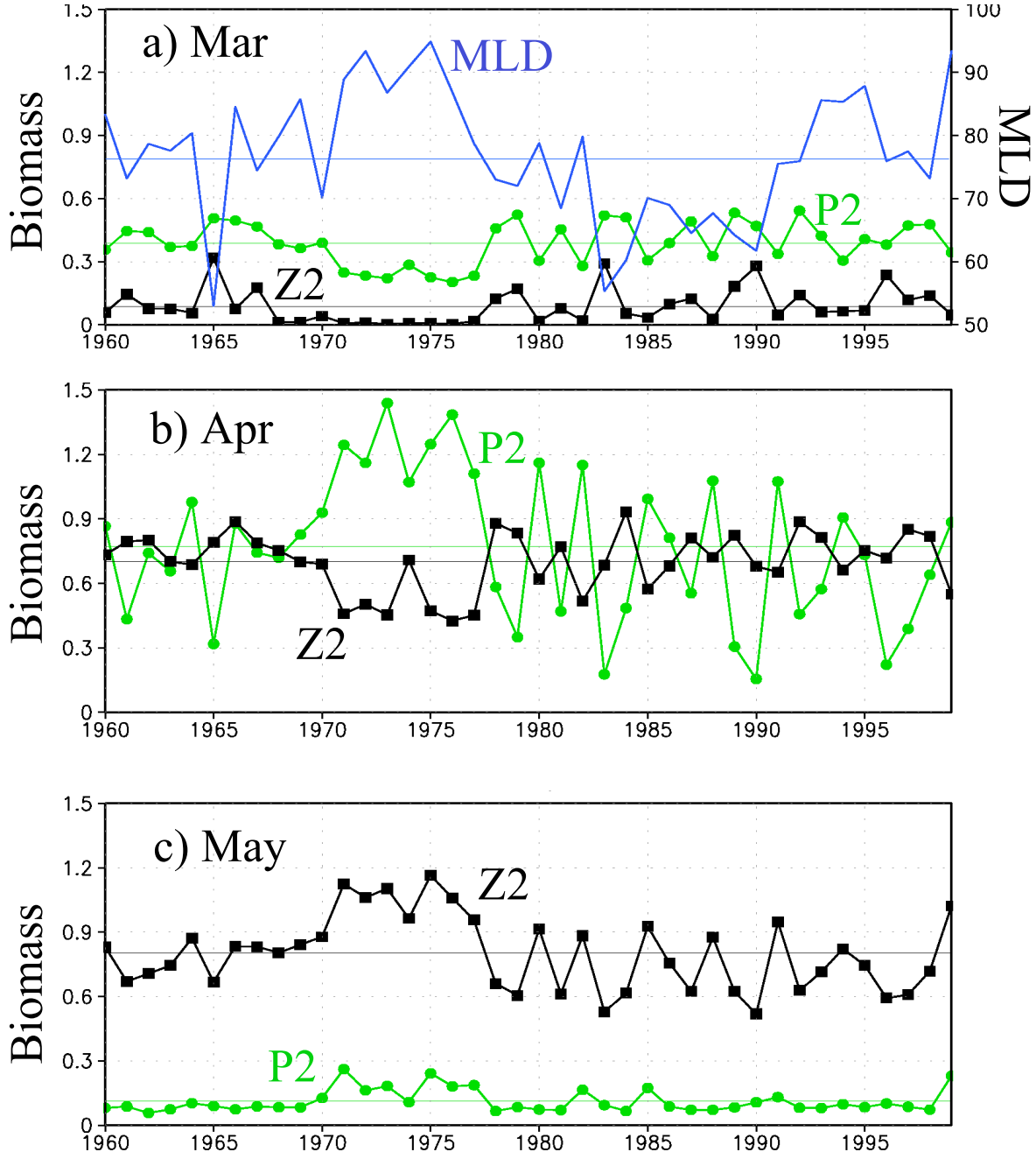

Scatter Plot of MLD, P2 and Z2 in GOA region

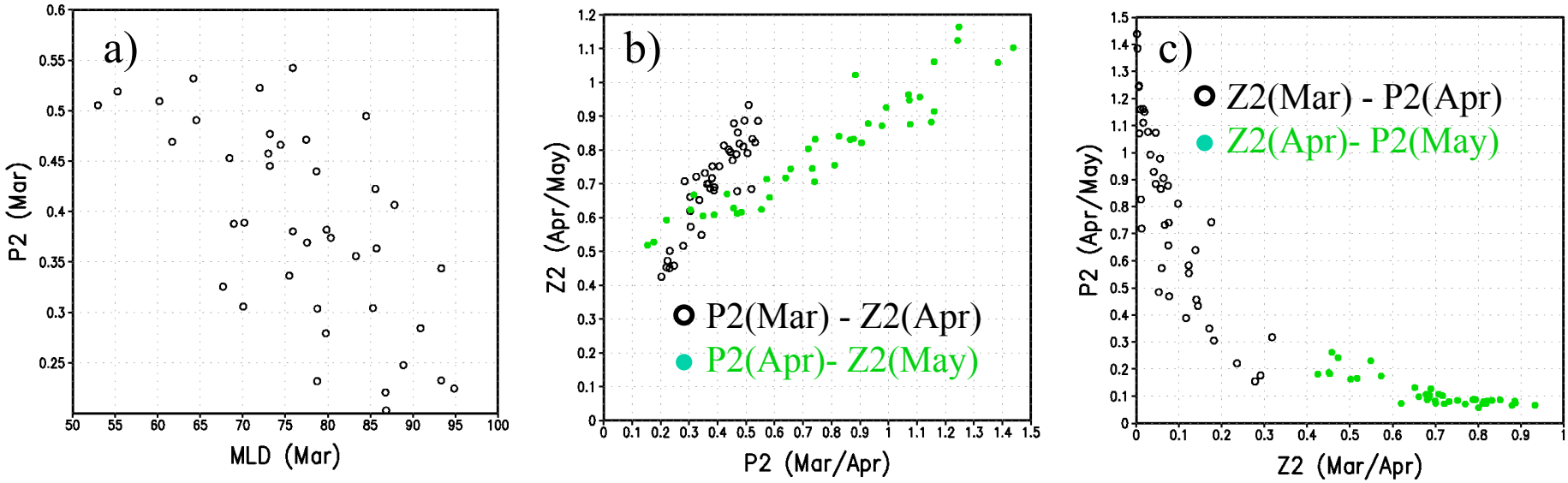

Fig. 10

MLD and Plankton Biomass Averaged 160ºW-140ºW
1977-88 (contours) 1977-88 - 1970-76 (shaded)

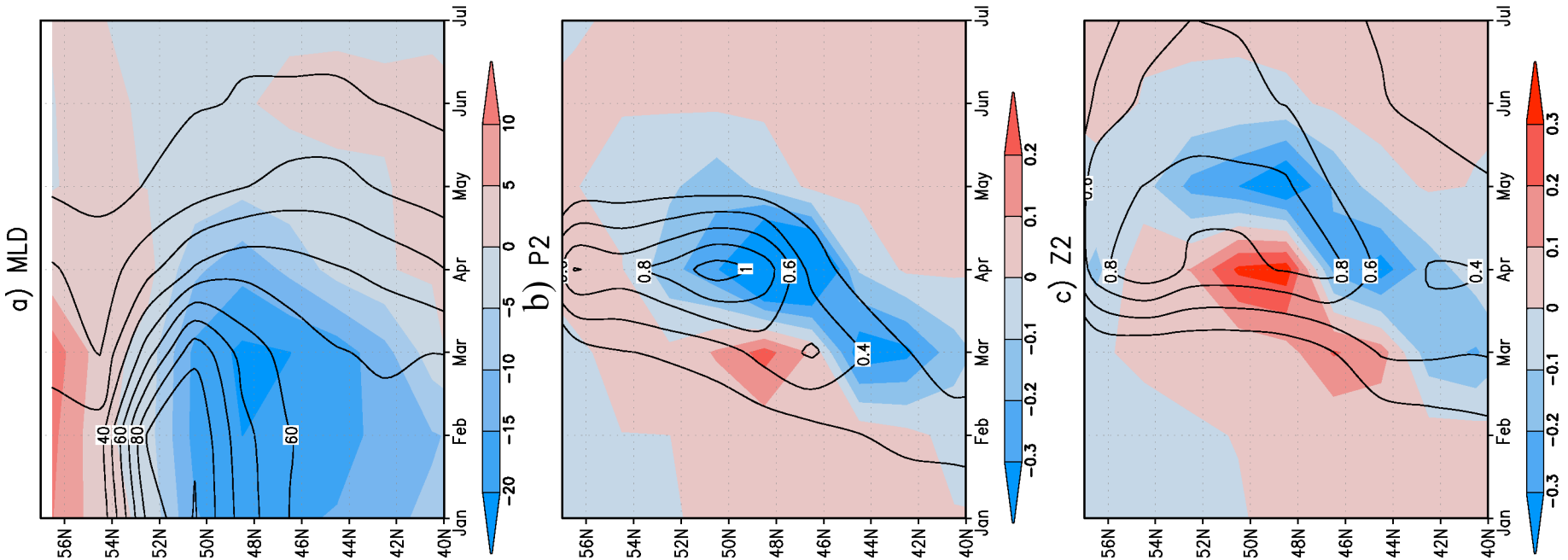

Fig. 11

Local 1 month Lead/Lag P-Z Correlations

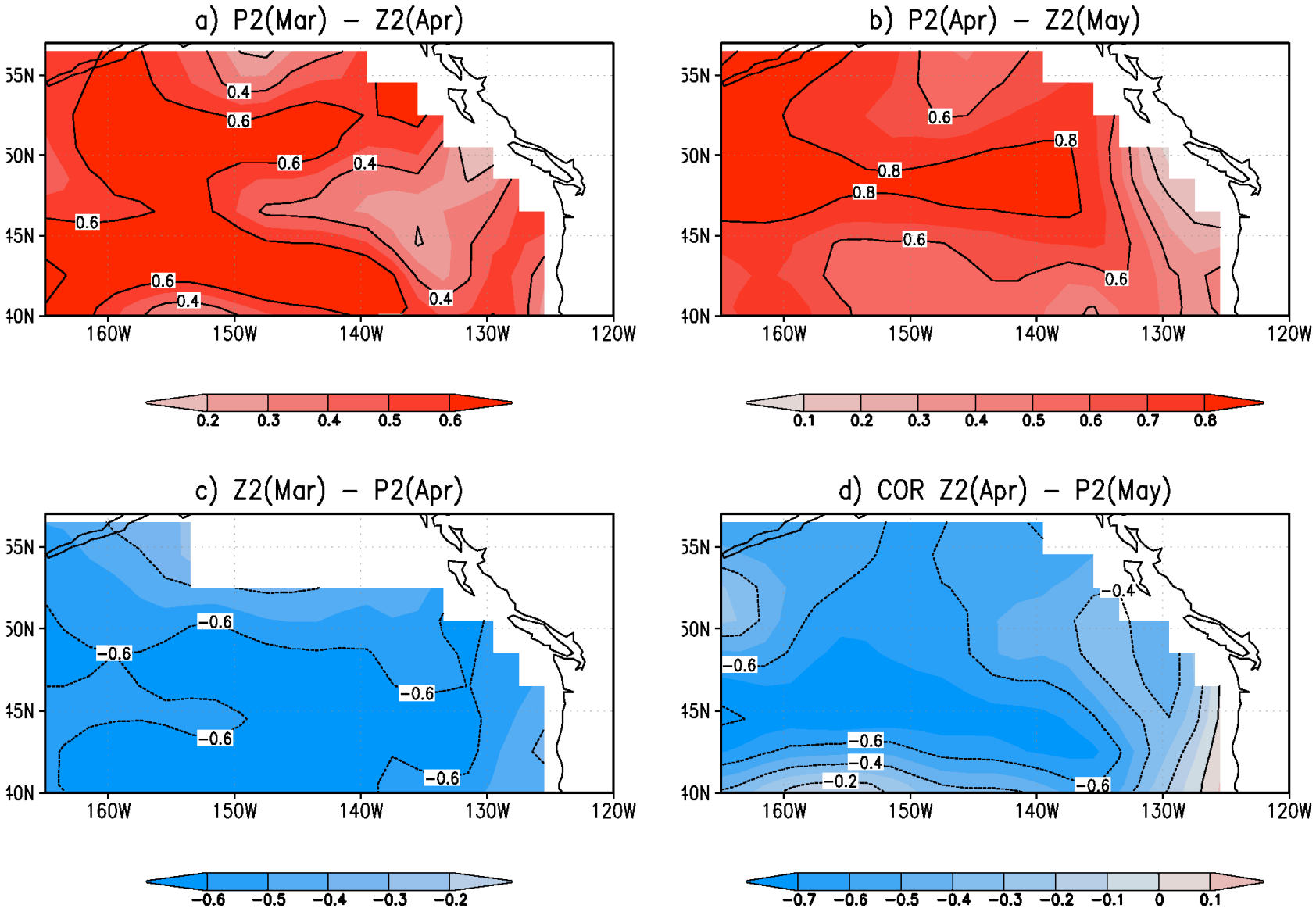

Fig. 12

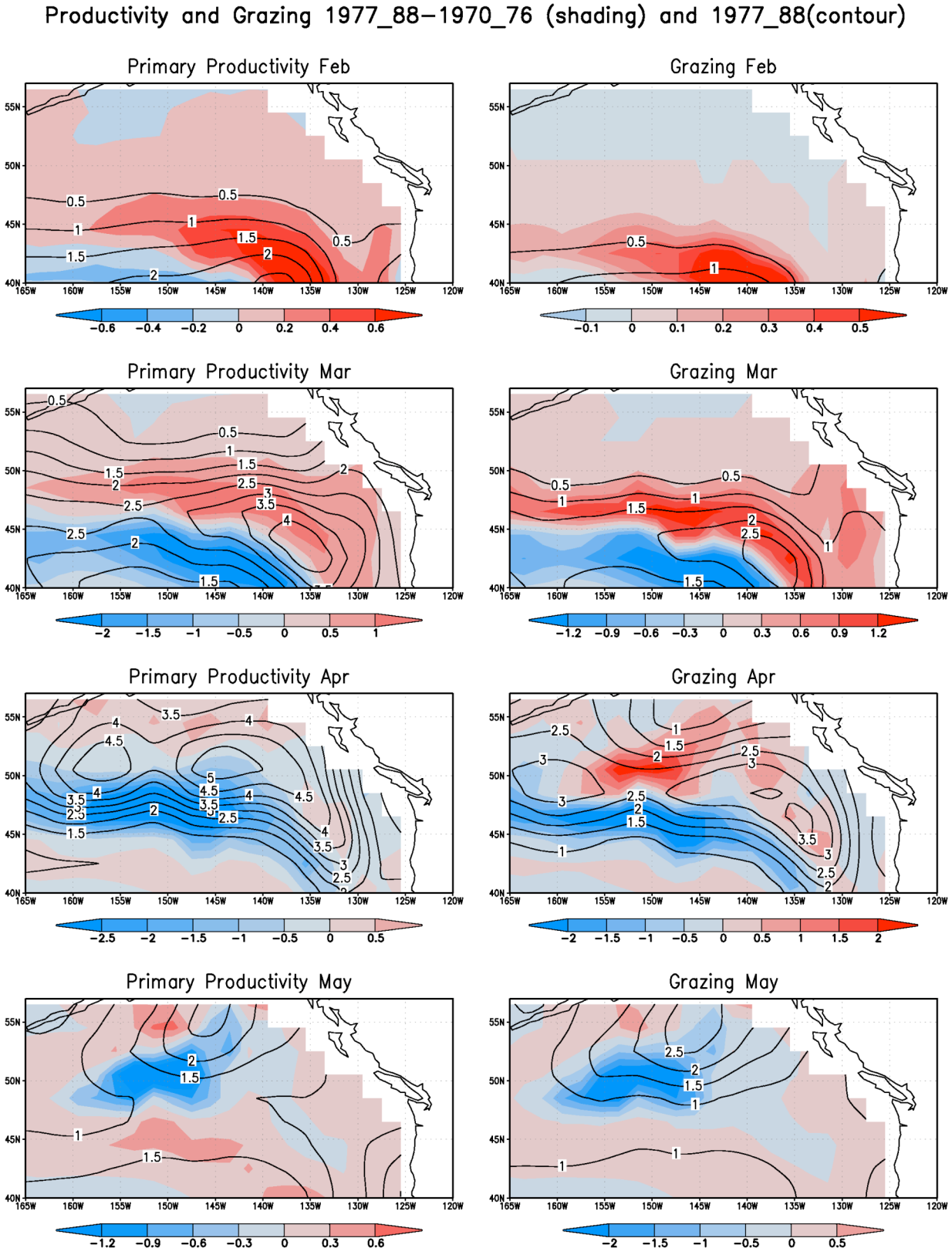

Fig 13: PP and Grazing